U. of MD PP#95-123

Exchange Current Corrections to Neutrino–Nucleus Scattering (I): Nuclear Matter

Y. Umino
Department of Physics, University of Maryland
*College Park, MD 20742-4111, U.S.A.**
and
National Institute for Nuclear and High–Energy Physics, Section K (NIKHEF–K),
Postbus 41882, NL–1009 DB Amsterdam, The Netherlands

J.M. Udias
National Institute for Nuclear and High–Energy Physics, Section K (NIKHEF–K),
Postbus 41882, NL–1009 DB Amsterdam, The Netherlands
(February 9, 2008)

Abstract

Relativistic exchange current corrections to the impulse approximation in low and intermediate energy neutrino–nucleus scattering are presented assuming non–vanishing strange quark form factors for constituent nucleons. Two–body exchange current operators which treat *all* $SU(3)$ vector and axial currents on an equal footing are constructed by generalizing the soft–pion dominance method of Chemtob and Rho. For charged current reactions, exchange current corrections can reduce the impulse approximation results by 5 to 10 % depending on the nuclear density. A finite strange quark form factor may change the total cross section for neutral current scattering by 20% while exchange current corrections are found to be sensitive to the nuclear density. Implications on the current LSND experiment to extract the strange quark axial form factor of the nucleon are discussed.

11.40.Ha, 24.80.Dc, 25.30.Pt

*Present address.

I. INTRODUCTION

The existence of two–body meson exchange currents (MEC) in electromagnetic and weak axial interactions in nuclei has by now been firmly established [1–3]. In the electromagnetic sector the need for two–body currents has been realized even before the discovery of the pion by Siegert in 1937 through his consideration of vector current conservation [4]. However, it took almost 35 years before the first solid quantitative evidence for MEC was discovered when the 10% discrepancy between theory and experiment in the threshold radiative np capture rates was remedied in terms of one–pion exchange current correction [5]. The explanation soon after of the cross section for the inverse reaction, the electrodisintegration of the deuteron, in terms of MEC [6] left little doubt of the important role that two–body currents play in electromagnetic interactions of the deuteron. For larger nuclei, it is well known that effects of MEC are best found in low and intermediate energy magnetic isovector processes. These two–body currents play important roles in realistic descriptions of diverse nuclear phenomena such as the renormalization of orbital g–factors, δg_l [7], magnetic form factors of light p-shell nuclei [8], transverse (e, e') response functions in the dip region [9–11] and cross–sections for electromagnetically induced two–nucleon emission reactions [12].

The role of MEC in weak axial transitions in nuclei has been investigated by Kubodera, Delorme and Rho [13] who predicted a large renormalization of axial charge due to two–body currents. An ideal place to test their prediction is in the first–order forbidden β–decays whose transition amplitude involves a cancellation between time and space components of the one–body nucleon current, thus making it sensitive to two–body MEC effects. Indeed, Guichon, Giffon and Samour [14] found that the impulse approximation prediction of the ratio of μ–capture to β–decay rates for the $0^+ \leftrightarrow 0^-$ transition between ^{16}O and ^{16}N was a factor of 2 larger than the measured value. This large discrepancy disappeared when they included two–body MEC corrections to the impulse approximation. In addition, recent shell model analysis of first forbidden β-decay rates covering a wide range of nuclei [15–17] indicates a substantial exchange current contribution to the renormalization of weak axial charge in nuclear medium, thus confirming the prediction of Kubodera, Delorme and Rho. These solid empirical evidences of two–body currents in electromagnetic and weak axial processes in low and intermediate energy nuclear phenomena strongly motivate to investigate whether charged and neutral currents, where both vector and axial currents are involved, are also subject to renormalizations in nuclei due to MEC.

Another reason to study MEC effects in low and intermediate energy neutrino–nucleus scattering is that it has been receiving increasing attention as a means to measure the strangeness matrix elements of the nucleon [18–25]. The measurement of polarized structure function g_1 and the extraction of the sum rule suggested the possibility of a rather large strange quark axial matrix element for the proton leading to the so–called "spin crisis" [26]. Although there are numerous works attempting to understand the role of hidden flavor in nucleons [27], the situation regarding the strangeness degrees of freedom in the nucleon is far from clear and it is hoped that neutral current neutrino–nucleus interactions might be able to shed a new light into this problem [28].

For example, Garvey *et al.* pointed out that the ratio of proton–to–neutron yield in quasi–elastic neutral current neutrino–nucleus scattering, hereafter denoted by $R(p/n) \equiv \sigma(\nu, \nu' p)/\sigma(\nu, \nu' n)$, is an observable that is sensitive to the strange axial form factor of the

nucleon [22,24]. This ratio is currently being measured in the LSND experiment at Los Alamos [22]. In their work Garvey *et al.* calculated $R(p/n)$ within a non-relativistic RPA framework using the impulse approximation and later included the effects of final state interactions experienced by the ejected nucleon with a continuum RPA formalism [24]. This correction was found to have about 30% effect on individual neutrino–nucleus cross sections but cancelled out in the ratio of proton–to–neutron yields. A similar calculation by Horowitz *et al.* [25] using a Relativistic Fermi Gas (RFG) model in the impulse approximation did not include the final state interactions but the resulting $R(p/n)$ was found to be similar to that of Garvey *et al.* However, in order to extract strangeness matrix elements of the nucleon from neutral current neutrino–nucleus scattering it is necessary to investigate the reliability of calculating the cross sections for this process by assuming finite strange quark form factors for the constituent nucleons. Previously, neutral and charged current neutrino–nucleus scattering have been investigated beyond the impulse approximation in [29] but without strange quark form factors and MEC corrections. In addition, this and other proposals [20,21] to extract strange quark form factors of the nucleon from neutrino–nucleus scattering involves kinematics ranging from low–energy inelastic scattering to the quasi-elastic region. Experience from electron scattering suggests that MEC corrections to neutrino–nucleus cross sections in this kinematic range might be important.

The same LSND collaboration has recently announced their measurement of the cross section for the inclusive charged current reaction $^{12}C(\nu_{\mu^-}, \mu^-)X$ near threshold [30] which is significantly lower than existing model predictions. This discrepancy is in some cases more than 100% [31] and it is conjectured that nuclear effects which are important in low–energy neutrino–nucleus interactions have been left out in these model calculations. One such effect is the MEC corrections to the impulse approximation and it is therefore interesting to explore whether two–body corrections to the one–body nucleon current will help to remedy this recently observed discrepancy.

Previously, MEC corrections have been investigated only in neutrino–deuteron reactions using non–relativistic kinematics and *without* assuming any strange quark form factors [32–35]. In a recent letter [36] a method to construct relativistic MEC operators applicable to neutrino–nucleus scattering was presented taking into account the possible finite strange quark form factors of nucleons. This method treats all the $SU(3)$ currents on the same footing and thus is able to estimate MEC corrections to electromagnetic as well as neutral and charged current processes simultaneously. It is also model independent in the sense that no underlying nucleon–nucleon interaction needs to be specified in order to construct the MEC operators. In this paper details of the method is presented together with examples of the use of the resulting MEC operators in electron and neutrino scatterings assuming nuclear matter and using the kinematics of the on–going LSND experiment. The focus of this paper is to investigate only the effects of exchange currents, and therefore a simple RFG model is used to model the target nucleus. In order to make a more realistic comparison with experiment additional nuclear effects must be incorporated in the description of the neutrino–nucleus scattering process. These effects will be considered in a forthcoming paper [37].

In the following section the problem is defined and empirical and theoretical motivations are presented for the use of the method originally developed by Chemtob and Rho to construct MEC operators [39]. Their formalism is then generalized to take into account finite

strange quark form factors and advantages of using the generalized method and assumptions made in constructing the MEC operators are discussed. Section III illustrates the usefulness of the generalized operators by evaluating two–body MEC corrections to quasi–elastic electron scattering as well as neutral and charged current neutrino scattering reactions. Finally, the results are summarized in the concluding section accompanied by Appendicies which present all the necessary formalism needed to evaluate the nuclear response functions in neutrino–nucleus scattering together with some new technical details.

II. EXCHANGE CURRENT OPERATORS FOR ALL CURRENTS

A. Currents and Form Factors

This section presents the construction of MEC operators applicable to both electron and neutrino–nucleus scattering by generalizing the method developed by Chemtob and Rho [39]. As will be shown below, this generalized method is able to estimate exchange current corrections to *any* linear combination of $SU(3)$ vector and axial currents given by

$$J_\mu(k) = \sum_{a=0}^{8} \Big(\alpha^a V_\mu^a(k) + \beta^a A_\mu^a(k) \Big) \tag{2.1}$$

where V_μ^a and A_μ^a are the $SU(3)$ vector and axial vector currents of the nucleon, respectively, and $k \equiv k_\mu$ is the four momentum of the incoming probe. The $SU(3)$ singlet ($a = 0$) and octet ($a = 1 \rightarrow 8$) currents are defined using the usual Pauli, $F_1^a(Q^2)$, Dirac, $F_2^a(Q^2)$, axial, $G_A^a(Q^2)$, and induced axial $H_A^a(Q^2)$ *on–shell* nucleon form factors where $Q^2 \equiv -k^2$

$$V_\mu^0(k) \equiv \sqrt{\frac{2}{3}} \Big[F_1^0(Q^2)\gamma_\mu + F_2^0(Q^2)\Sigma_\mu \Big] \mathbf{I} \tag{2.2}$$

$$V_\mu^i(k) \equiv \Big[F_1^i(Q^2)\gamma_\mu + F_2^i(Q^2)\Sigma_\mu \Big] \lambda^i \tag{2.3}$$

$$A_\mu^0(k) \equiv \sqrt{\frac{2}{3}} \Big[G_A^0(Q^2)\gamma_\mu\gamma_5 + H_A^0(Q^2)k_\mu\gamma_5 \Big] \mathbf{I} \tag{2.4}$$

$$A_\mu^i(k) \equiv \Big[G_A^i(Q^2)\gamma_\mu\gamma_5 + H_A^i(Q^2)k_\mu\gamma_5 \Big] \lambda^i \tag{2.5}$$

Here $i = 1 \rightarrow 8$, λ^i are the usual Gell-Mann matrices normalized to Tr $(\lambda^a\lambda^b) = 2\delta_{ab}$, $\mathbf{I}$ is the identity matrix and the magnetic operator Σ_μ is defined as

$$\Sigma_\mu \equiv \frac{i}{2M}\sigma_{\mu\nu}k^\nu \tag{2.6}$$

with M being the free nucleon mass. Thus, the problem addressed in this paper is to estimate two–body MEC corrections to the general one–body $SU(3)$ nucleon current shown in Eq. (2.1) when the nucleon is immersed in nuclear medium. Once this is accomplished, MEC operators corresponding to electromagnetic, weak axial, neutral and charged currents may be trivially constructed by taking the appropriate linear combinations.

For example, the one–body nucleon electromagnetic current is recovered when $\alpha^3 = 1$ and $\alpha^8 = 1/\sqrt{3}$ and by letting the remaining coefficients vanish, multiplied by the appropriate isoscalar and isovector electric charges, *i.e.*

$$J_\mu^{EM} \propto \left(V_\mu^3 + \frac{1}{\sqrt{3}} V_\mu^8\right) \tag{2.7}$$

Similarly, one–body neutral, $J_\mu^{Z^0}$ and charged, $J_\mu^{W^\pm}$, currents are given by the following linear combinations of vector and axial currents [19]

$$J_\mu^{Z^0} \propto V_\mu^3 - A_\mu^3 - 2\sin^2\theta_W \left(V_\mu^3 + \frac{1}{\sqrt{3}} V_\mu^8\right) - \frac{1}{2}\left(V_\mu^0 - \frac{2}{\sqrt{3}} V_\mu^8\right) + \frac{1}{2}\left(A_\mu^0 - \frac{2}{\sqrt{3}} A_\mu^8\right) \tag{2.8}$$

$$J_\mu^{W^\pm} \propto \left[\left(V_\mu^1 \pm i V_\mu^2\right) - \left(A_\mu^1 \pm i A_\mu^2\right)\right]\cos\theta_C + \left[\left(V_\mu^4 \pm i V_\mu^5\right) - \left(A_\mu^4 \pm i A_\mu^5\right)\right]\sin\theta_C \tag{2.9}$$

In these definitions of neutral and charged currents, θ_W and θ_C are the Weinberg and Cabbibo angles, respectively, and small QED, QCD and heavy quark corrections to $J_\mu^{Z^0}$ [19] as well as contributions from the charmed quarks to $J_\mu^{W^\pm}$ are ignored. Note that the third term in Eq. (2.8) is proportional to the electromagnetic current, Eq. (2.7), while the last two terms are referred to as the strange vector, V_μ^s, and axial, A_μ^s, currents of the nucleon.

$$V_\mu^s \equiv V_\mu^0 - \frac{2}{\sqrt{3}} V_\mu^8 \tag{2.10}$$

$$A_\mu^s \equiv A_\mu^0 - \frac{2}{\sqrt{3}} A_\mu^8 \tag{2.11}$$

For neutral current processes where only massless leptons are involved, the induced axial form factor does not contribute to the total cross section and therefore is not determined. At $Q^2 = 0$, the strange quark Pauli form factor $F_1^s \equiv F_1^0 - 2/\sqrt{3}F_1^8$ vanishes by definition and only F_2^0 and G_A^0 are unknown among the form factors in Eqs. (2.2)–(2.5). According to the Standard Model, these two form factors determine the strange quark magnetic, $F_2^s \equiv F_2^s(0)$, and axial, $G_A^s \equiv G_A^s(0)$, form factors of the nucleon. In this work all form factor parametrizations are taken from [38] which are the same ones used in [22]. Specifically, the Q^2 dependence of $F_2^s(Q^2)$ and $G_A^s(Q^2)$ are

$$F_2^s(Q^2) \equiv F_2^0(Q^2) - \frac{2}{\sqrt{3}} F_2^8(Q^2) \tag{2.12}$$

$$G_A^s(Q^2) \equiv G_A^0(Q^2) - \frac{2}{\sqrt{3}} G_A^8(Q^2) \tag{2.13}$$

where

$$F_2^{0,8}(Q^2) \equiv \frac{F_2^{0,8}(0)}{(1 + \frac{Q^2}{4M_N^2})(1 + \frac{Q^2}{M_V^2})^2} \tag{2.14}$$

$$G_A^{0,8}(Q^2) \equiv \frac{G_A^{0,8}(0)}{(1 + \frac{Q^2}{M_A^2})^2} \tag{2.15}$$

In these definitions the vector and axial masses are set to $M_V = 840$ MeV and $M_A = 1030$ MeV, respectively, and the octet form factors at $Q^2 = 0$ are $F_2^8(0) \equiv \sqrt{3}/2(\kappa_p + \kappa_n)$ and $G_A^8(0) \equiv \sqrt{3}/6(3F - D)$.

B. Soft–Pion Exchange Dominance and the Chiral Filter Hypothesis

Although empirical evidences abound suggesting that both one–body electromagnetic and weak axial currents are renormalized in nuclear medium by MEC, there still lacks a rigorous theoretical understanding of the roles that different types of MEC might play in nuclei. For example, in electromagnetic processes any conserved transverse MEC consistent with a given $N-N$ interaction is acceptable since it is not constrained by the Ward–Takahashi identity. A typical "brute force" approach of estimating MEC effects in electro–nuclear phenomena is to choose a model dependent $N-N$ interaction in the one–boson exchange approximation and from this interaction construct the MEC operators with a longitudinal component satisfying the Ward–Takahashi identity and a corresponding conserved transverse component. In addition, in applications to many–body systems it is necessary to construct nuclear wave functions *from the same* $N-N$ interaction including the Fock term to maintain self–consistency. This latter requirement is often neglected without any justifications especially in relativistic calculations. The situation in the weak axial case is more ambiguous since there are no conservation laws to constrain the form of MEC operators except in the chiral limit. Thus, it is desirable to identify the important contributions from a multitude of two–body currents involving exchanges of different types of mesons by exploiting some underlying physical principles. Fortunately, there has been some promising experimental and theoretical progress over the past 20 years towards accomplishing this goal.

In 1978, Kubodera, Delorme and Rho [13], using the method developed by Chemtob and Rho to be described below, have argued that, *in the absence of kinematical suppressions*, MEC processes in low and intermediate energy nuclear phenomena are dominated by one–pion exchange whose production amplitude is evaluated in the soft–pion limit. In another words, they stressed that dominant contribution to the two–body correction arises from MEC which are consistent with nuclear force implied by chiral symmetry, other short–ranged meson exchanges being "filtered out" by the nuclear medium. Thus, the crucial element in their argument is the important role played by chiral symmetry in nuclei, a key symmetry manifest in QCD. Using this so–called *chiral filter hypothesis*, they arrived at the prediction of axial charge renormalization which subsequently was confirmed through the analysis of first forbidden β–decay rates as mentioned in the introductory section. In general, Kubodera, Delorme and Rho found that MEC derived assuming soft–pion dominance approximation, hereafter referred to as soft–pion MEC, strongly renormalizes the time component of axial currents and the space component of electromagnetic currents, respectively.

The idea of soft–pion dominance has been applied in the past to various low and intermediate energy phenomena and proved to be a viable technique in estimating exchange current corrections. For example, in their analysis of first forbidden β–decay rates Warburton *et al.* compared the use of the soft–pion exchange dominance approximation to other MEC operators and found that both methods can reproduce the observed enhancement of the axial charge [16,17]. The successful application of soft–pion MEC operators here is not surprising since β–decays typically involve small momentum transfers where the soft–pion dominance approximation is expected to apply. The real surprise came when the success of this approximation manifested itself in the electromagnetic sector. Initially, Riska and Brown [5] used the soft–pion MEC operators as prescribed by Chemtob and Rho to explain the difference between the impulse approximation prediction and the measured threshold

radiative *np* capture rates. The same method was employed by Hockert *et al.* [6] to calculate the cross section for the electrodisintegration of the deuteron which involved small energy ($E_{np} \approx 3$MeV) but *large* momentum transfers. They were able to reproduce the measured cross section up to momentum transfer of $k_\mu^2 = 10$ fm^{-2} using only the soft–pion MEC operators. Addition of the Δ resonance contribution had little effect on their original correction to the impulse approximation. The same cross section was later measured at Saclay [40] extending the momentum transfer up to $k_\mu^2 = 18$ fm^{-2}. The surprise came when the original prediction by Hockert *et al.* managed to reproduce the Saclay data up to $k_\mu^2 = 15$ fm^{-2} [41]. In this case different corrections to the soft–pion MEC cancelled each other leaving the original two–body contribution to be the dominant correction to the impulse approximation. Thus, there are concrete empirical evidences to support the use of the soft–pion dominance approximation in low and intermediate energy electromagnetic and weak axial interactions in nuclei.

Recently, Rho [42] has proposed an explanation for the success of the soft–pion MEC dominance based on Weinberg's derivation of nuclear forces from chiral Lagrangians [43,44]. Using chiral power counting arguments Rho has shown that to the leading order, *i.e.* at the tree level, the short range part of two–body MEC corresponding to a nuclear force predicted by a given chiral Lagrangian is considerably suppressed. Thus, the dominant contribution to the two–body correction to the impulse approximation comes from the long ranged part of the exchange current represented by the soft–pion exchange. Subsequently, Park, Towner and Kubodera [45] have calculated next–to–leading order corrections to the axial charge MEC operators beyond the soft–pion dominance approximation using heavy fermion chiral perturbation theory. They found that loop corrections to the soft–pion MEC operators are of the order of 10%, and argued that their results are consistent with the claims of Warburton *et al.* and support the chiral filtering conjecture. Thus, not only are there empirical evidences suggesting the renormalization of electromagnetic and weak axial currents by MEC in nuclei, but there also exists theoretical motivations to believe that this renormalization is dominated by soft–pion exchange interaction, at least up to momentum transfers of about one GeV [41,42].

C. Soft–Pion MEC Operators

The method of Chemtob and Rho to construct soft–pion MEC operators [39] is based on soft–pion theorems and current algebra techniques pioneered by Adler [46]. Here, this method is generalized to accommodate *all* the $SU(3)$ currents appearing in Eq. (2.1) and the main advantage of using this technique to estimate MEC corrections to neutrino–nucleus scattering is pointed out. Since the derivation of soft–pion MEC operators may be found in the original works of Adler [46] and Chemtob and Rho [39], and the generalization to $SU(3)$ being straightforward, most of the technical details are relegated to Appendix B.

In the soft–pion dominance approximation, the operator representing an exchange of a pion between two nucleons is written as products of the pion production amplitude by an external current off the first nucleon, the pion propagator and the matrix element for pion absorption by the second nucleon

$$J_\mu^a(k; P_{I,1}; P_{I,2}; P_{F,1}; P_{F,2})_{EX} =$$

$$\frac{1}{(2\pi)^4}\delta^4(P_{I,1}+P_{I,2}+k-P_{F,1}-P_{F,2})\langle N(P_{F,1})\pi^b(q)|J^a_\mu(k)|N(P_{I,1})\rangle$$
$$\times\frac{i}{q^2-m_\pi^2}\langle N(P_{F,2})|J^b_\pi(q)|N(P_{I,2})\rangle+(1\leftrightarrow 2) \qquad (2.16)$$

Here the matrix element $\langle N(P_{F,1})\pi^b(q)|J^a_\mu(k)|N(P_{I,1})\rangle$ is the amplitude for pion production off a nucleon by an external vector or axial $SU(3)$ current $J^a_\mu(k)$, $J^a_\mu(k)+N(P_{I,1})\rightarrow\pi^b(q)+N(P_{F,1})$, where $q\equiv q_\mu$ is the four momenta of the produced pion. a and b are $SU(3)$ indices with $a=0\rightarrow 8$ to accommodate all the $SU(3)$ currents and $b=1$, 2 or 3 for pion production. Similarly, $\langle N(P_{F,2})|J^b_\pi(q)|N(P_{I,2})\rangle$ is the matrix element for pion absorption by a nucleon using the pseudoscalar πNN coupling

$$\langle N(P_{F,2})|J^b_\pi(q)|N(P_{I,2})\rangle=g_{\pi NN}\,\langle N(P_{F,2})|\gamma_5\lambda^b|N(P_{I,2})\rangle \qquad (2.17)$$

Note the absence of πNN form factor in Eq. (2.17). It is quite remarkable that the present method can describe the electrodisintegration data involving momentum transfers of up to about $k^2_\mu=15$ fm^2 without the use of any πNN form factors in the πNN absorption vertex.

To construct soft–pion MEC operators it is necessary to know the pion production amplitude in Eq. (2.16) in the soft–pion limit of $q\rightarrow 0$. In this limiting procedure it is necessary to first take the spatial part of the four vector to zero in order to select the long range, *i e.* the S–wave, part of the $N-N$ interaction and *then* take the chiral limit of $q_0\rightarrow 0$. The resulting amplitude, originally derived by Adler [46] using the PCAC hypothesis

$$\partial^\mu A^a_\mu=m^2_\pi F_\pi\pi^a \qquad (2.18)$$

and used by Chemtob and Rho in [39] has the following form when generalized to the $SU(3)$ formalism

$$\lim_{q\rightarrow 0}\langle N(P_F)\pi^b(q)|J^a_\mu(k)|N(P_I)\rangle=\frac{i}{F_\pi}\int d^4x\lim_{q\rightarrow 0}(-iq^\mu)\langle N(P_F)|T\left(A^b_\mu(x)J^a_\mu(0)\right)|N(P_I)\rangle \qquad (2.19)$$
$$-\frac{i}{F_\pi}\langle N(P_F)|\left[Q^b_5(x),J^a_\mu(0)\right]_{x_0=0}|N(P_I)\rangle$$

Here $Q^a_5(x)\equiv\int d^3xA^a_0(x)$ is the axial charge. As shown in [47], the only contributions to the first term in the soft–pion limit come from pole diagrams where the axial current A_μ is inserted in the external lines in the amplitude $\langle N(P_F)|J^a_\mu(k)|N(P_I)\rangle$ and thus behaving as $1/q_\mu$. The second term may be simplified by using the $SU(3)\otimes SU(3)$ current algebra

$$\left[Q^a_5(x),V^b_\mu(0)\right]_{x_0=0}=if_{abc}A^c_\mu(0) \qquad (2.20)$$
$$\left[Q^a_5(x),A^b_\mu(0)\right]_{x_0=0}=if_{abc}V^c_\mu(0) \qquad (2.21)$$

and has no contributions from singlet currents unlike in the first term where both $SU(3)$ singlet and octet can contribute. Therefore, the amplitude for soft–pion emission in the reaction $N(P_I)\rightarrow N(P_F)$, in the presence of perturbation $J^a_\mu(k)$, may be expressed in terms of two matrix elements $\langle N(P_F)|J^a_\mu(k)|N(P_I)\rangle$ and $\langle N(P_F)|\left[Q^b_5(x),J^a_\mu(0)\right]_{x_0=0}|N(P_I)\rangle$. Since J^a_μ may be any one of vector or axial $SU(3)$ currents, Eq. (2.16) may simultaneously be

applied to all the components of the general one–body $SU(3)$ current in Eq. (2.1), and specifically to the electromagnetic current of Eq. (2.7) as well as to neutral and charged currents of Eqs. (2.8) and (2.9), respectively. Thus, it is the use of $SU(3) \otimes SU(3)$ current algebra in Eq. (2.20), which rotates around the vector and axial currents, that makes the generalized method of Chemtob and Rho particularly suitable to approximate MEC corrections in neutrino–nucleus scattering at low and intermediate energies. In addition, because the soft–pion limit is taken no $N - N$ interaction needs to be specified and the present method of constructing MEC operators only requires the currents in the impulse approximation as inputs. In this sense the present approach to constructing MEC operators is model independent. Note also that the present method is valid *to all orders* in $g_{\pi NN}$ in one of the πNN verticies since the pion production amplitude Eq. (2.20) is evaluated non–perturbatively [46].[1]

It is useful to discuss the approximations made in calculating the soft–pion production amplitudes. Since the original application of soft–pion theorems has been on pion photo–production processes, these amplitudes have been evaluated by assuming that the initial and final nucleons are on their mass shell. However, in order to construct MEC operators in nuclei consistently it is necessary to take both the initial and the final nucleons off their mass shell. This involves density dependent off–shell parametrizations of nucleon currents which are not known. In fact, a fully consistent many–body description of in–medium nucleon electromagnetic or weak form factors has never been presented. Considering this lack of understanding of off–shell modification of nucleon form factors and currents in nuclear medium, the most reasonable approximation to make is the use of on–shell kinematics and parametrizations of nucleon form factors as has been done in all previous works involving MEC in nuclei. This implies that the nucleons are assumed to obey the free Dirac equation, and therefore in the derivation of the pion production amplitude $\not{p}u(\vec{p})$ has been replaced with $Mu(\vec{p})$, where $u(\vec{p})$ is the nucleon spinor with three momentum $\vec{p}$ and mass M. This on–shell approximation is used from the very beginning, even before considering the soft–pion limit, and is consistent with using the *free* RFG model of the nucleus to calculate the cross sections where the constituent nucleons are assumed to be on–shell.

Related to the derivation of soft–pion production amplitudes, Eq. (2.20), is the use of PCAC and pion off–shell extrapolation. When using the PCAC relation, it is assumed that the matrix element of the divergence of the axial current varies smoothly and *slowly* with the pion mass q^2. In addition it is also assumed that this matrix element is approximately proportional to the pion field and that any dependence on higher order non-linear pion field terms are negligible. This assumption allows one to make a connection between the results obtained with $q \approx 0$ with a more realistic value of q^2. Since a zero four momentum pion is not a physical object, this slow q^2 variation assumption is always needed to compare the soft–pion predictions with experiment. Finally, the soft–pion production amplitudes are valid only to zeroth order in q. This means that if there are any processes contributing to

[1]The expressions for the soft–pion production amplitudes presented in Appendix B are proportional to $g_{\pi NN}$. However, this does not mean that the amplitudes are evaluated to first order in $g_{\pi NN}$. The πNN coupling constant was introduced through the use of the Goldberger–Trieman relation [46].

the pion production which, for kinematical reasons, are of first order in q, the applications of current algebra and soft-pion techniques used here give no information about them. In order to describe these processes, it is necessary to make a model dependent analysis of specific reactions which requires the introduction of a $N-N$ interaction.

Relativistic $SU(3)$ soft–pion MEC operators are constructed in analogy with the method outlined in [39] and are listed in Appendix B. The conservation of the vector current has been checked analytically using the prescription discussed in the original paper by Adler [46] and verified numerically . To illustrate the usefulness of the present technique, soft–pion MEC corrections are applied to quasi–elastic electromagnetic, neutral and charged current interactions simultaneously in the following section. In this paper a simple RFG model formalism [48,49] is used for all calculations without binding energy corrections ($B = 0$). Finite nucleus effects, final state interactions and other density dependent nuclear medium effects are not considered on purpose in order to clearly isolate the effects of soft–pion MEC in many body systems.

III. RESULTS

A. Quasi–Elastic Electron Scattering

As mentioned in Section IIA, the third term in the expression for the one–body neutral current of the nucleon, Eq. (2.8), is proportional to the electromagnetic current, $J_\mu^{EM} \propto V_\mu^3 + \frac{1}{\sqrt{3}} V_\mu^8$. Thus, estimates of MEC effects in electron scattering can automatically be extracted when calculating two–body corrections to neutral current processes using the formalism under consideration. The successful application of the soft–pion MEC approximation to the electrodisintegration of the deuteron has been described in the previous section. Here, the same method is applied to quasi–elastic electron scattering off heavier nuclei where many–body effects, not present in the reaction involving the deuteron, are expected to play important roles.

In Figures 1a and 1b, separated longitudinal, $R_L(\omega, |\vec{k}\,|)$, and transverse, $R_T(\omega, |\vec{k}\,|)$, response functions for a typical quasi–elastic inclusive $^{12}C(e,e')$ reaction are shown as a function of energy transfer ω both in the impulse approximation and with soft–MEC corrections. A Fermi momentum of $k_F = 225$ MeV and a fixed three momentum transfer of $|\vec{k}\,| = 400$ MeV are used in the RFG model of the nucleus without any binding energy corrections ($B = 0$) so that the nucleons in the target nucleus are *on–shell*. Since the momentum transfer is almost twice the Fermi momentum, the influence of Pauli blocking should be small in this kinematical range and indeed, as shown in the figures, the small effect of Pauli blocking is manifested in the linear dependence of the response functions for small ω [48]. Thus, the RFG model of the nucleus is adequate as a first approximation to test the soft–pion dominance approximation. Only $1p1h$ final states are considered when evaluating the MEC matrix elements since they are the dominant two–body contributions to the response functions in the quasi–elastic region. A more quantitative two–body MEC corrections to electron scattering at these energies, and especially in the dip region, would require model dependent Δ propagation and pion production processes as pointed out in [9,10]. Also shown in the figures for reference are the experimental data for the same inclusive electron scattering reaction measured at Saclay [50]. *However, no attempt has been made to fit the*

data by varying k_F and B, since the vector currents will no longer be conserved with a finite binding energy correction and the target nucleons will be off their mass shell.

As shown in Figure 1a, the MEC correction to the impulse approximation in the longitudinal response results in a small reduction of the quasi–elastic peak with no appreciable change in the peak position. However, this reduction of the impulse approximation result is too small to describe the magnitude of the quasi–elastic peak observed in the Saclay data. This feature persists even if k_F and B are varied in an attempt for a better fit to the data. The failure of the free Fermi Gas model to describe the observed longitudinal response in quasi–elastic inclusive electron scattering for a wide range of nuclei is well–known [51], and additional nuclear effects must be incorporated in order to improve the present model calculation. Also shown in the figure is the individual soft–pion MEC contribution which is small and negative resulting in the small reduction of the quasi–elastic peak.

For the transverse response shown in Figure 1b, the soft–pion MEC correction can increase the magnitude of the quasi–elastic peak by about 20% relative to the impulse approximation results and shift the peak position to a lower value of energy transfer ω by about 20 MeV. These effects of the two–body current correction may be understood by examining the individual soft–pion MEC contribution which causes both constructive and destructive interferences depending on the value of the energy transfer. This contribution is positive between $\omega = 0$ and 125 MeV and negative thereafter and results in an increase of the magnitude of the quasi–elastic peak and a shift of the peak position to a lower value of ω. The qualitative agreement with data is better than in the longitudinal response although the observed peak position can not be reproduced with zero binding energy correction ($B = 0$). A finite value of the binding energy will help to shift the quasi–elastic peak towards the observed position but, as mentioned above, the total electromagnetic current will no longer be conserved in this case. Thus, two–body soft–pion MEC corrections to inclusive electron scattering response functions tend to slightly soften the longitudinal response and leads to about 20% increase in the transverse response in the free RFG model.

It is interesting to compare the present results with numerous model calculations of R_L and R_T in the literature. However, to make any quantitative comparisons with other works are very difficult since many model dependent assumptions have been made for each of the calculations which are hard to disentangle. For example, Kohno and Ohtsuka [52] also investigate the MEC corrections to the inclusive electron scattering response functions in the quasi–elastic region considering only the $1p1h$ final states. In contrast to the present work, they work in the non–relativistic approximation and ignore contributions of order greater than $g^2_{\pi NN}$. The method adopted in this paper is fully relativistic and one of the πNN verticies is valid to all orders in $g_{\pi NN}$. Also, they include the Δ excitation current which has a strong model dependence as well as the "pion–in–flight" MEC, referred to as "pionic" MEC in their paper. As discussed in Appendix B, the pion–in–flight diagram does not contribute to the (e, e') response functions since it is proportional to the four momentum transfer of the leptonic probe, k_μ, in the soft–pion limit. Nevertheless, there is qualitative agreement between the soft–pion MEC contribution shown in Figures 1a and 1b and their corresponding "pion pair" MEC results presented in Figure 2b of [52]. It is interesting to note that in their calculation for the longitudinal response, there is a cancellation between the "pionic" and Δ excitation MEC corrections leaving the "pair" current the dominant correction to the impulse approximation as in Figure 1a of the present paper. This is not

true for their transverse response where Kohno and Ohtsuka find that the total effect of the two–body corrections is to decrease the impulse approximation result which is the opposite effect shown in Figure 1b. The reason for this discrepancy is due to the large negative contribution from their Δ excitation current which is not included in the present work. It should be noted that another RFG model calculation of R_T that includes the same types of MEC corrections as in Kohno and Ohtsuka [10], but considers only the $2p2h$ final states, obtains an increase in the transverse response since the $2p2h$ matrix elements are added incoherently to the impulse approximation result. Thus, unlike the case of the deuteron, it is difficult to make a definitive statement on the success of the application of soft–pion MEC dominance approximation in electron scattering off nuclei by comparing with other works, except to say that the results presented above are not inconsistent with other model calculations.

B. Quasi–Elastic Charged Current Neutrino Scattering

The one–body charged current, Eq. (2.9), is the next simplest linear combination of $SU(3)$ vector and axial currents of physical interest after the electromagnetic current discussed above. Since the nucleon has no *net* strangeness ($F_1^s(Q^2 = 0) = 0$), only the term proportional to $\cos\theta_C$ in Eq. (2.9) contributes to the charged current neutrino–nucleus scattering cross sections. Although no direct information regarding the strange quark form factors of the nucleon may be obtained in charged current processes, these reactions are nevertheless important in extracting the value of the axial mass parameter M_A which appears in the parametrization of axial form factors. Recently, the LSND collaboration has reported on their measurement of neutrino flux–averaged inclusive ${}^{12}C(\nu_{\mu^-}, \mu^-)X$ cross section of (8.3 $\pm$ 0.7 stat. $\pm$ 1.6 syst.)$\times 10^{-40}$ cm^2 in the neutrino energy region of $123.7 < E_\nu < 280$ MeV with a flux–weighted average of $< E_\nu > = 180$ MeV [30]. This value is substantially smaller than an earlier measurement, which used a different neutrino energy distribution, of (15.9 $\pm$ 2.6 stat. $\pm$ 3.7 syst.)$\times 10^{-39}$ cm^2 [53] as well as predictions from model calculations [31]. Because these cross sections are measured just above the muon threshold energy, it is expected that nuclear effects will substantially modify the impulse approximation predictions. MEC corrections is one such effect and its impact on the impulse approximation calculation is examined in this subsection using the soft–pion dominance formalism.

In contrast to the charged current reaction involving the muon–neutrino, it is interesting to note that there is good agreement between model predictions and the measured cross section for the exclusive charged current reaction ${}^{12}C(\nu_e, e^-)N_{g.s.}$ involving *electron*–neutrinos [54]. From the computational point of view, the main difference between electron– and muon–neutrino induced charged current reactions is that in the former case, the mass of the outgoing electron is negligible while the muon mass has to be explicitly included for the latter case. This means that in the charged current reaction ${}^{12}C(\nu_{\mu^-}, \mu^-)X$, the term proportional to the induced axial form factor, $H_A(k^2)$, will contribute to the total cross section. In the present formalism, the induced axial form factor is given by PCAC in the pion pole dominance

$$H_A(k^2) = G_A(0)\frac{2M}{k^2 - m_\pi^2} \tag{3.1}$$

where $G_A(0) \equiv g_A/2 = 1/2(F+D)$ is the axial coupling constant. However, because of the presence of the $H_A(k^2)$ term there is an ambiguity when applying current conservation to the vector currents. The prescription given by Adler in [46] has been used here to insure vector current conservation and details are given in Appendix B.

Figure 2 shows the total cross section for the inclusive charged current process $^{12}C(\nu_{\mu^-},\mu^-)X$ for several nuclear densities obtained by folding the LSND neutrino energy distribution [30,55]. As in the electron scattering case, the RFG model without binding energy corrections is used to model the nucleus and only $1p1h$ final states are considered when taking matrix elements of two–body operators since the phase space for $2p2h$ final states should be suppressed due to the rather low energy neutrino beam [55]. However, because the flux–weighted average of the neutrino beam energy is $< E_\nu > = 180$ MeV, the three momentum transfers are twice smaller than in the electron scattering reaction discussed above and consequently, the effect of Pauli blocking becomes more important in this charged current reaction. In the RFG model of the nucleus an increase in nuclear density is equivalent to an increase in the Fermi momentum. Thus, with a constant neutrino beam energy the net effect of Pauli blocking is the decrease of the total cross–section *per nucleon* with increasing nuclear density as shown in Figure 2. In the impulse approximation, the total cross section decreases from 24 to 13 ($\times 10^{-40}$cm^2) as the Fermi momentum is varied from $k_F = 220$ to 300 MeV. As shown in the figure, the inclusion of soft–pion MEC corrections reduces the impulse approximation results by 5 to 10% as the Fermi momentum is increased from 220 to 300 MeV. For $k_F = 225$ MeV, which is the usual value used for ^{12}C, the total cross section is reduced from 24.1 to 22.7 ($\times 10^{-40}$cm^2). This reduction is not enough to explain the recently measured value reported by the LSND collaboration.

In Figure 3a, the $^{12}C(\nu_{\mu^-},\mu^-)X$ cross section is shown as a function of neutrino energy for $k_F = 225$ MeV including Coulomb corrections for the outgoing muon. Corrections from two–body currents to the impulse approximation are very small and difficult to observe. Note that the muon production threshold is found to be around 107 MeV compared to the experimental threshold of 124 MeV. This is because the present RFG calculation does not include any binding energy corrections which will ruin the vector current conservation. Corresponding calculation using non–relativistic continuum RPA formalism [31] obtained a smaller cross section which increases more slowly with the neutrino energy. The effect of soft–pion MEC is more evident when the differential $^{12}C(\nu_{\mu^-},\mu^-)X$ cross section folded with the experimental neutrino energy distribution is plotted against the muon kinetic energy, E_μ, as shown in Figure 3b. Corrections from two–body currents are largest near the cross section peak around $E_\mu = 23$ MeV where the impulse approximation result of 43.7×10^{-42} cm^2/MeV is reduced to 40.1×10^{-42} cm^2/MeV. However, these corrections become less important with increasing muon kinetic energy and for $E_\mu > 60$ MeV there is hardly any change from the impulse approximation result. The results shown in Figure 3b are qualitatively consistent with non–relativistic Fermi Gas and continuum RPA results shown in [31] although various model dependent assumptions, such as a different neutrino energy distribution, prevents from a direct quantitative comparison between these results. Thus, although the two–body soft–pion MEC corrections help to reduce the impulse approximation prediction of the exclusive charged current reaction $^{12}C(\nu_{\mu^-},\mu^-)X$ towards the observed value, this reduction is not enough and additional nuclear structure effects are required to further lower the total cross section for this exclusive process [56,57]. These additional effects will be incorporated in a

future work [37].

C. Quasi–Elastic Neutral Current Neutrino Scattering

The final application of the soft–pion MEC correction is in the quasi–elastic neutral current neutrino–nucleus scattering where the one–body neutral current of the constituent nucleon is given by Eq. (2.8). This particular linear combination of the general $SU(3)$ current of Eq. (2.1) is interesting since, unlike the electromagnetic and charged currents, it includes the $SU(3)$ vector and axial *singlet* currents leading to a possible strange quark contribution to the neutrino–nucleus scattering reaction. Also, in contrast to the charged current reactions, the term proportional to the induced axial form factor H_A does not contribute to the neutral current neutrino–nucleus cross section since the leptons involved in the scattering process are massless. In Eq. (2.8), the strange quark electric form factor F_1^s is assumed to be vanishingly small for small values of virtuality that are of interest here, and therefore only magnetic, F_2^s and axial G_A^s strange quark form factors of the nucleon are used to describe the contributions from the strange sea quarks in neutral current neutrino–nucleus scattering. In the following discussion these two strange quark form factors are treated as input parameters and no attempt has been made to determine their values from model calculations. As in the preceeding discussions on electromagnetic and charged current reactions, all the calculations are performed using the RFG model without binding energy corrections.

In Figure 4, differential cross sections for the $^{12}C(\nu, \nu' p)$ reaction, $d\sigma/dE_F$, where E_F is the total energy of the ejectile, are shown in the quasi–elastic region as functions of the ejected proton's kinetic energy, T_F, for several values of Fermi momenta. The incident neutrino energy is assumed to be 200 MeV and the values used for the strange magnetic and axial quark form factors are $F_2^s = -0.21$ and $G_A^s = -0.19$, respectively. The long dashed curves are the impulse approximation results while the solid curves have been obtained with the soft–pion MEC corrections, and as in the charged current case, only $1p1h$ final states have been taken into account. In the impulse approximation, the magnitude of the peak decreases from about 70 to 53 ($\times 10^{-42}$ cm^2/MeV) as k_F is varied from 200 to 350 MeV. However, this decrease is accompanied by a redistribution of the strength to higher values of T_F in such a way that the area under the differential cross section remains approximately a constant since it is roughly proportional to the number of nucleons which is fixed. Note that because the incident neutrino energy is constant and small, the position of the maximum of the differential cross section is approximately the same at around T_F=30 MeV despite the decrease in the peak magnitude. This means that the effect of Pauli blocking becomes very important when computing the *total* cross section obtained by integrating the differential cross section $d\sigma/dE_F$ for $E_F > E_{Fermi}$, thereby cutting off the contributions around the peak magnitude. This total cross section decreases noticeably with increasing k_F, as it was the case for the total charged current cross section shown in Figure 2.

It is evident from the figures that the soft–pion MEC effects are sensitive to the nuclear density in this model calculation. For k_F around 200 MeV, there is very little difference between the impulse approximation and the MEC corrected results due to an important cancellation to be discussed below. This cancellation becomes less complete with increasing k_F and the two–body current effects become stronger and decreases the impulse approximation results with increasing nuclear density as shown in the figures. This effect of the

soft–pion MEC on the impulse approximation persists when the strange quark form factors are assumed to vanish ($F_2^s = G_A^s = 0$) in the model calculation. However, without any strange quark form factors there is a large reduction in the differential cross section for protons as shown in Figure 5. In this figure k_F is set to 225 MeV and there is little correction coming from the exchange currents in the soft–pion approximation for this value of Fermi momentum. Note that the magnitude of the quasi–elastic peak is reduced from about 70 to 50 $\times 10^{-42}$ cm^2/MeV when the strange quark magnetic and axial form factors are varied from $F_2^s = -0.21$ to $F_2^s = 0$ and $G_A^s = -0.19$ to $G_A^s = 0$, respectively. For the neutral current induced *neutron* knockout reaction, $^{12}C(\nu, \nu' n)$, a finite strange quark form factor decreases the differential cross section relative to that obtained without any strange quark distribution for nucleons [22,25].

It is instructive to understand why the soft–pion exchange current corrections are small for neutral current scattering for nuclear densities corresponding to $k_F \approx 200$ MeV. As shown in Appendix A Eq. (A38), the differential cross section *per nucleon* for neutral current scattering in the RFG model is given by a linear combination of three structure functions W_L, W_T and W_{TT} as

$$\left(\frac{d\sigma^{Z^0}}{dE_F}\right)_{\rm RFGM} = \left(\frac{3\pi}{4k_F^3}\right) \int_0^{k_F} d\epsilon_f d(\cos\theta)\, \frac{\sigma^{Z^0}}{|\vec{k}\,|} \Big[\omega_L W_L + \omega_T W_T + \omega_{TT'} W_{TT'}\Big] \tag{3.2}$$

Here ω_L, ω_T and $\omega_{TT'}$ are the kinematical coefficients corresponding to the longitudinal W_L, transverse W_T and transverse–transverse $W_{TT'}$ structure functions, respectively. In Figure 6 the individual contributions from these three structure functions to the differential cross section are shown using the same parameters as in Figure 5. Note that all three contributions to $d\sigma/dE_F$ are positive, the dominant one coming from the transverse term $\omega_T W_T$ followed by the transverse–transverse $\omega_{TT'} W_{TT'}$ and the longitudinal $\omega_L W_L$ terms, the latter contributing negligiblely to the differential cross section. Note that the soft–pion MEC correction increases the $\omega_{TT'} W_{TT'}$ term and decreases the $\omega_T W_T$ term relative to their impulse approximation results leading to a cancellation of MEC effects for this particular value of Fermi momentum. This cancellation between the transverse and transverse-transverse contributions becomes less and less complete as the nuclear density is increased and the effect of two–body correction becomes bigger for higher densities as shown in Figure 4. Eq. (3.2) can also be used to understand the behaviour of the differential cross section for *anti–neutrino* scattering relative to the neutrino induced nucleon knockout rates as follows.

Figure 7 shows the $d\sigma/dE_F$ for the neutral current anti–neutrino scattering reaction $^{12}C(\bar{\nu}, \bar{\nu}' p)$ and the corresponding neutrino reaction both of which are obtained again by using the same input parameters as in Figure 5. In the impulse approximation, the magnitude of the quasi–elastic peak for anti–neutrino scattering is approximately half that of the neutrino scattering, the former value being 38 $\times 10^{-42}$ cm^2/MeV compared to 70 $\times 10^{-42}$ cm^2/MeV for the latter. Also, the position of the peak is shifted towards a lower value of T_F by about 10 MeV relative to the neutrino scattering case. The effect of soft–pion MEC corrections to the impulse approximation result for anti–neutrino scattering is noticeably larger than the corresponding correction for neutrino scattering for nuclear densities corresponding to $k_F = 225$ MeV as shown in the figure. For the $^{12}C(\bar{\nu}, \bar{\nu}' p)$ reaction, the impulse approximation result for the magnitude of the quasi–elastic peak is reduced from 38 to 30 $\times 10^{-42}$ cm^2/MeV, while there is no such noticeable reduction for the neutrino scattering.

Thus, not only the anti–neutrino scattering differential cross section greatly reduced relative to neutrino scattering, but the effect of soft–pion MEC on the impulse approximation result is much bigger reducing further the $d\sigma/dE_F$ by about 15%.

This difference in the neutrino and anti–neutrino differential cross sections may be understood by once again examining Figure 6 and noting the definitions of the structure functions W_i and their corresponding kinematical coefficients ω_i given in Eqs. (A15) to (A29) of Appendix A. The only difference between the longitudinal, transverse and transverse–transverse structure functions and kinematical coefficients entering in Eq. (3.2) for the neutrino and anti–neutrino scattering is in the sign of $\omega_{TT'}$ given by Eq. (A28). Therefore, the graph corresponding to Figure 6 for anti–neutrino scattering will have a negative transverse–transverse contribution which partially cancels the dominant transverse contribution yielding the small differential cross section as shown in Figure 7. In addition, because the $\omega_{TT'}W_{TT'}$ term is now negative, the MEC correction to this term will further decrease the correction to the transverse term resulting in a non–negligible two–body correction to the differential cross section not observed in the neutrino scattering case. Hence although the differential cross section for the anti–neutrino reaction $^{12}C(\bar{\nu},\bar{\nu}'p)$ is about half that of the corresponding neutrino scattering reaction, its impulse approximation result is subject to non–negligible soft–pion MEC corrections.

In the Introduction it was mentioned that the ratio of proton–to–neutron yields in quasi–elastic neutral current scattering, $R(p/n)$, is currently being measured in the LSND experiment to extract the value of the strange quark axial form factor, G_A^s. In this experiment the probing neutrinos and anti–neutrinos are incident on a tank of mineral water composed of hydrogen and carbon molecules [22]. The amount of kinetic energy carried by the struck nucleon is measured by the detectors surrounding the tank of mineral water and $R(p/n)$ is determined as a function of the detected ejectile's kinetic energy, T_F. The proton–to–neutron ratio is then integrated over T_F and compared with model predictions which gives the integrated $R(p/n)$ as a function of G_A^s for several values of the strange quark magnetic form factor as shown in Figure 8. However, in practice there is an experimental cutoff in the range of T_F, given by 50 MeV $< T_F <$ 120 MeV, in order to make sure that the detected protons are knocked out from the carbon nucleus. The RFG model calculation of the ratio of integrated proton–to–neutron yields of Figure 8 is qualitatively similar to the ratios predicted by a non–relativistic RPA calculation [22] and shows only about a few percent change from the impulse approximation results in the ratio for the neutrino scattering while this change is about 10% for anti–neutrinos. The latter change originates in the non–negligible two–body correction to the impulse approximation in the anti–neutrino scattering reaction explained in the preceeding paragraph. In both cases, the two–body corrections tend to decrease the integrated ratio and this effect increases as G_A^s becomes less and less negative for a given value of F_2^s. For example, if $G_A^s \approx -0.1$, the soft–pion MEC corrections are negligible for the neutrino scattering $R(p/n)$ for all physically relevant values of F_2^s but must be taken into account in analyzing the anti–neutrino scattering ratio. Finally, final state interaction effects should be examined within a relativistic framework, although it is known from a non-relativistic calculation [24] that the effects on the integrated ratios are almost negligible.

IV. DISCUSSION

In this work relativistic two–body MEC corrections have been applied simultaneously to quasi–elastic electromagnetic and neutrino scattering reactions using a single unified formalism obtained by generalizing the method developed by Chemtob and Rho [39]. The basic strategy employed here is to use the chiral filtering hypothesis [13,41] which assumes that the two–body MEC correction in nuclei is dominated by the exchange of a single pion whose production amplitude is evaluated in the soft–pion limit. By assuming PCAC and using the $SU(3) \otimes SU(3)$ current algebra this soft–pion dominance approximation allows one to express the pion production amplitudes in terms of $SU(3)$ vector and axial currents interacting with the nucleon. Thus the resulting MEC operators are expressed in terms of currents used in the impulse approximation without any references to model dependent $N-N$ interaction. These soft–pion MEC operators arise from the longest range (*i.e.* the S–wave) part of the $N-N$ interaction and PCAC is used to relate the soft–pion predictions to experiment. This is the reason why it is necessary to take the spatial part of the pion four momentum to zero first when taking the $q_\mu \to 0$ limit. The generalized version of the method of Chemtob and Rho used in this work is so far the most economical way to estimate exchange current corrections to low and intermediate energy neutrino–nucleus scattering since it treats all the $SU(3)$ vector and axial currents in Eq. (2.1) on the same footing, and is a natural way to accommodate the strange quark vector and axial currents of the nucleon allowed by the Standard Model.

Previously, the non–relativistic and $SU(2)$ version of the soft–pion MEC operators have been successfully applied to first forbidden β–decays [13,15–17] and to electromagnetic and neutrino scattering off few nucleon systems [5,34,35,39] including processes involving large momentum transfers [6]. This last phenomenological success came as a real surprise since the soft–pion MEC operators were expected to be applicable only to those processes involving small momentum transfers such as in β–decays. It led to speculations [41] that the physics in nuclei is dominated by processes dictated by chiral symmetry and a theoretical justification was proposed [42] to explain the phenomenological success by extending the work of Weinberg [44] on nuclear forces derived from chiral Lagrangians [42]. Motivated by these developments, fully relativistic $SU(3)$ soft–pion MEC operators have been used to estimate two–body corrections to the impulse approximation in quasi–elastic electromagnetic and neutrino scattering reactions assuming a finite magnetic and axial strange quark form factors of the nucleon. In order to clearly isolated the effect of two–body corrections in many body systems, a simple free RFG model of the target nucleus was used without any other medium dependent corrections.

The inclusive (e, e') longitudinal and transverse response functions in the quasi–elastic region obtained using MEC corrections show a small reduction of the impulse approximation result for the longitudinal channel while a substantial increase was observed for the transverse response. The former result is in qualitative agreement with a previous work using non–relativistic kinematics [52], while the relativistic MEC corrections tend to increase the response function in the transverse channel in contradiction to the results of [52] but in agreement with another relativistic calculation [10,11]. It should be stressed that in almost all calculations of MEC corrections in electron scattering reactions, such as in [10,52], the one–pion exchange operators are of order $g^2_{\pi NN}$ whereas the MEC operators used in this

work is valid to all orders in $g_{\pi NN}$ at one of the πNN verticies since the soft–pion production amplitude is evaluated non–perturbatively [46]. Thus it is difficult, if not impossible, to make any quantitative comparisons with other works dealing with MEC corrections in electron scattering especially if additional medium corrections are present in a given calculation. However, in order to make a more quantitative prediction it is necessary to introduce these nuclear medium effects, such as density dependent nucleon mass and form factors, as well as MEC involving the excitation of the Δ resonance. For these reasons, the most successful application of soft–pion MEC correction in electromagnetic interactions is still in the electrodisintegration of the deuteron investigated over 20 years ago.

The charged current neutrino–nucleus reaction investigated in the present work is the inclusive $^{12}C(\nu_{\mu^-},\mu^-)X$ reaction where the total cross section has recently been measured by the LSND experiment [30]. In the RFG model calculation, the two–body soft–pion exchange correction reduces the impulse approximation result for the cross section by 5 to 10 % as the Fermi momentum is increased from 200 to 300 MeV. For $k_F = 225$ MeV, a typical Fermi momentum used for ^{12}C, the total cross section is reduced from 24.1 to 22.7 ($\times 10^{-40}$cm^2) which is not enough to explain the recently measured value reported by the LSND collaboration of (8.3 $\pm$ 0.7 stat. $\pm$ 1.6 syst.)$\times 10^{-40}$cm^2 [30]. Recall that the previously reported measurement is (15.9 $\pm$ 2.6 stat. $\pm$ 3.7 syst.)$\times 10^{-39}$cm^2 [53] which was measured using a different neutrino energy distribution than in the LSND experiment. If the LSND measurement is correct, then some important density dependent physics is responsible for the large reduction of the impulse approximation result, a situation reminiscent of the "missing strength" problem in the longitudinal (e,e') response functions of the last decade [51].

The quasi–elastic neutral current induced nucleon knockout reaction $^{12}C(\nu,\nu' N)$ is currently being investigated by the LSND collaboration in an effort to extract G_A^s by measuring the ratio of proton–to–neutron yields. For the proton knockout reaction, the impulse approximation result for the differential cross section is found to be sensitive to the values of strange quark form factors of the nucleon, while the two–body soft–pion correction becomes more important as the nuclear density is increased. However, for densities appropriate for ^{12}C the MEC corrections to the structure functions cancel each other resulting in small changes from the impulse approximation results. Because of this cancellation the ratio of proton–to–neutron yield for neutrino scattering does not suffer from two–body corrections and, at the present level of sophistication, the impulse approximation result is sufficient to describe the ratio $R(p/n)$. The corresponding knockout reaction involving anti–neutrinos exhibits a much smaller differential cross section than in the neutrino scattering case and a non–negligible MEC correction to the impulse approximation result. These differences may be understood by once again examining the contributions from different structure functions to the differential cross section. In this case, one of the kinematical coefficients corresponding to a structure function changes sign relative to the neutrino scattering case. As a result, there is a cancellation in the impulse approximation results leading to a reduced differential cross section but an enhancement in the magnitude of the MEC correction which amounts to about 10–15% of the impulse approximation result depending on the value of G_A^s. However, in order to make a concrete statement about the extraction of the strange quark axial form factor from the measured $R(p/n)$, additional nuclear effects, such as final state interactions, need to be considered in addition to MEC corrections.

In this paper, motivated by the LSND neutrino scattering experiment, the quasi–elastic region in electron and neutrino scattering was chosen to apply the soft–pion MEC corrections. This kinematic regime probably represents the limit of the applicability of the soft–pion dominance approximation as presented in this work. Description of processes involving larger momentum transfers would involve the introduction of the Δ excitation current, pion production processes as well as short ranged meson exchanges. There exists prescriptions to extend the present technique to incorporate these processes as shown in [34,35] albeit in the non–relativistic $SU(2)$ formalism. It would be interesting to extend these prescriptions to the present relativistic $SU(3)$ formalism since it can trivially be used to estimate MEC corrections to *any* linear combination of $SU(3)$ axial and vector currents shown in Eq. (2.1). For example, the extended formalism may be used to investigate parity violating electron scattering processes which involves the interference of electromagnetic and weak neutral currents. Other phenomena of interest to examine are neutral current scattering of solar and supernova neutrinos off deuterons [34] assuming finite strange quark form factors for the nucleons and inelastic nuclear transitions which can only take place in the presence finite strange quark form factors [20]. The latter investigation would involve a relativistic finite nucleus neutrino scattering calculation which is the subject of the upcoming paper.

ACKNOWLEDGMENTS

YU would like to thank S. Krewald, C. Horowitz and K. Langanke for stimulating discussions at their home institutes during the early stages of this work. YU was supported by the foundation for Fundamental Research of Matter (FOM) and the Dutch National Organization for Scientific Research (NWO). YU also acknowledges support from US Department of Energy under grant No. DE–FG02–93ER–40762. JMU is carrying out the work as a part of a Community training project financed by the European Commission under Contract ERBCHBICT 920185.

APPENDIX A: CONVENTIONS AND FORMULAE

In this Appendix conventions and formulae used to compute semi–inclusive differential cross–sections for neutral and charged current neutrino–nucleus reactions in the RFG model are summarized for completeness. Because the technical details for including the $1p1h$ and $2p2h$ MEC contributions to the hadronic tensor in the Fermi Gas models are given in detail in [9,11], only the impulse approximation results are presented here. Although these references deal only with electron scattering, generalization to both charged and neutral current neutrino scattering is straightforward. Conventions of Halzen and Martin [58] are used throughout.

As usual, it is assumed that the target nucleus consists of A nucleons with mass M_A and that a single nucleon is ejected from the target due to the interaction with the probe. In what follows M is the mass of the free nucleon and the initial and final four momenta of the ejectile, $P_I^\mu \equiv (E_I, \vec{P}_I)$ and $P_F^\mu \equiv (E_F, \vec{P}_F)$, are related to the four momentum transfer to the target k^μ by $P_I^\mu = k^\mu - P_F^\mu$. Incoming and outgoing lepton four momenta are denoted

by $k_i^\mu \equiv (\epsilon_i, \vec{k}_i)$ and $k_f^\mu \equiv (\epsilon_f, \vec{k}_f)$, respectively. A positive energy nucleon with energy E in a plane wave state is given by

$$\psi^\sigma_{PW}(\vec{P}, \vec{r}\,) = \frac{e^{i\vec{P}\cdot\vec{r}}}{\sqrt{2EV}}\, u(\vec{P}, \sigma) \tag{A1}$$

where the 4–component spinor $u(\vec{P}, \sigma)$, normalized to $u^\dagger u = 2E$, is

$$u(\vec{P}, \sigma) = \sqrt{E + M} \begin{pmatrix} 1 \\ \dfrac{\vec{\sigma}\cdot\vec{P}}{E+M} \end{pmatrix} \chi^\sigma \tag{A2}$$

Here χ^σ is the usual 2-component Pauli spinor with spin index σ and the plane waves are normalized in a box of volume V such that

$$\int_V d\vec{r}\, (\psi^\sigma_{PW})^\dagger \psi^\sigma_{PW} = 1 \tag{A3}$$

The transition matrix element for the neutrino–nucleus scattering reaction is given in the usual way in the limit of very heavy vector boson masses (*i.e.* $m^2_{Z^0,W^\pm} \gg k^2$) as

$$S_{fi} = ig^2 \int d^4x \int d^4y \int \frac{d^4k}{(2\pi)^3}\, e^{ik_\alpha (x-y)^\alpha}\; j^\mu(\vec{x}\,) J_\mu(\vec{y}\,) \tag{A4}$$

where $j^\mu(\vec{x}\,)$ and $J_\mu(\vec{y})$ are the leptonic and hadronic currents, respectively, and the coupling constant g is defined as $g^2 \equiv G_F/\sqrt{2}$. The spatial parts of the leptonic and hadronic currents in the above transition matrix are

$$j^\mu(\vec{x}\,) = \frac{1}{2V} \frac{e^{i(\vec{k}_i - \vec{k}_f)\cdot\vec{x}}}{(\epsilon_i \epsilon_f)^{1/2}}\, \bar{u}(\vec{k}_f, \sigma_f) \gamma_\mu (1 \mp \gamma_5) u(\vec{k}_i, \sigma_i) \tag{A5}$$

$$J^\mu(\vec{y}\,) = \frac{1}{2V} \frac{e^{i(\vec{P}_I - \vec{P}_F)\cdot\vec{y}}}{(E_I E_F)^{1/2}}\, \bar{u}(\vec{P}_F, \sigma_F) \hat{J}^\mu(k) u(\vec{P}_I, \sigma_I) \tag{A6}$$

The minus and plus signs in Eq. (A5) correspond to neutrino and anti–neutrino scattering, respectively. In the impulse approximation, the hadronic current operator $\hat{J}^\mu(k)$ is given by either Eq. (2.8) for the neutral current or by Eq. (2.9) for the charged current, while the corresponding two–body MEC operators are discussed in Appendix B. The resulting cross section for *free* nucleons is given by

$$\left(d\sigma^{Z^0/W^\pm}\right)_{\rm Free} = \delta^{(4)}(k_i^\mu - k_f^\mu + P_I^\mu - P_F^\mu)\, \sigma^{Z^0/W^\pm} \frac{1}{4\epsilon_f^2 E_I E_F}\, \omega_{\mu\nu} W^{\mu\nu}\, d^3\vec{P}_F d^3\vec{k}_f \tag{A7}$$

where σ^{Z^0} and $\sigma^{W^\pm}$ assume the following form for neutral and charged current processes

$$\sigma^{Z^0} = 16\, \epsilon_f^2 \cos^2(\theta/2) \left[\frac{g^2}{4\pi}\right]^2 \tag{A8}$$

$$\sigma^{W^\pm} = 16 k_f^2 \left[\frac{g^2}{4\pi}\right]^2 \tag{A9}$$

with θ being the lepton polar scattering angle. The quantity $\omega_{\mu\nu}W^{\mu\nu}$ appearing in Eq (A7) may be expressed as a linear combination of various nuclear structure functions W_i as

$$\omega_{\mu\nu}W^{\mu\nu} = \omega_L W_L + \omega_T W_T + \omega_{TT} W_{TT} + \omega_{LT} W_{LT} + \omega_{LT'} W_{LT'} + \omega_{TT'} W_{TT'} \tag{A10}$$

These structure functions are most conveniently expressed in a coordinate system defined by the following orthogonal unit vectors

$$\hat{z} \equiv \hat{k} \tag{A11}$$

$$\hat{n}_\perp \equiv \frac{\vec{k} \times \vec{P}_F}{|\vec{k} \times \vec{P}_F|} \tag{A12}$$

$$\hat{n}_\parallel \equiv \frac{\hat{n}_\perp \times \vec{k}}{|\hat{n}_\perp \times \vec{k}\,|} \tag{A13}$$

In this coordinate system the spatial part of the hadronic current $\vec{J}$, where $J^\mu \equiv (\rho, \vec{J}\,)$, may be written as

$$\vec{J} = J_\parallel \hat{n}_\parallel + J_\perp \hat{n}_\perp + J_k \hat{k} \tag{A14}$$

Then the structure functions for the semi–inclusive neutral current $(\nu, \nu' N)$ reaction are

$$W_L = |\rho|^2 + \frac{\omega^2}{|\vec{k}\,|^2}|J_k|^2 - \frac{\omega}{|\vec{k}\,|}\, 2Re\,(\rho^* J_k) \tag{A15}$$

$$\omega_T W_T = \omega_\perp W_\perp + \omega_\parallel W_\parallel \tag{A16}$$

$$W_\perp = |J_\perp|^2 \tag{A17}$$

$$W_\parallel = |J_\parallel|^2 \tag{A18}$$

$$W_{TT} = \sin(2\phi_F) Re\,(J_\perp J_\parallel^\dagger) \tag{A19}$$

$$W_{LT} = Re\left[\Big(\rho - \frac{\omega}{|\vec{k}\,|}J_k\Big)\Big(-\sin\phi_F J_\perp^\dagger + \cos\phi_F J_\parallel^\dagger\Big)\right] \tag{A20}$$

$$W_{TT'} = Im\,(J_\parallel J_\perp^\dagger) \tag{A21}$$

$$W_{LT'} = Im\left[\Big(\rho - \frac{\omega}{|\vec{k}\,|}J_k\Big)\Big(\sin\phi_F J_\parallel^\dagger + \cos\phi_F J_\perp^\dagger\Big)\right] \tag{A22}$$

where ϕ_F is the azimuthal angle of the ejected nucleon. The kinematical coefficients ω_i corresponding to these structure functions are as follows

$$\omega_L = 1 \tag{A23}$$

$$\omega_\perp = \tan^2(\theta/2) - \Big[1 + \cos(2\phi_F)\Big]\left(\frac{k_\mu^2}{2|\vec{k}\,|^2}\right) \tag{A24}$$

$$\omega_\parallel = \tan^2(\theta/2) - \Big[1 - \cos(2\phi_F)\Big]\left(\frac{k_\mu^2}{2|\vec{k}\,|^2}\right) \tag{A25}$$

$$\omega_{TT} = \frac{k_\mu^2}{|\vec{k}\,|^2} \tag{A26}$$

$$\omega_{LT} = -2\sqrt{\tan(\theta/2) - \frac{k_\mu^2}{|\vec{k}\,|^2}} \tag{A27}$$

$$\omega_{TT'} = \mp 2\tan(\theta/2)\sqrt{\tan(\theta/2) - \frac{k_\mu^2}{|\vec{k}\,|^2}} \tag{A28}$$

$$\omega_{LT'} = \pm 2\tan(\theta/2) \tag{A29}$$

In the expressions for the coefficients $\omega_{TT'}$ and $\omega_{LT'}$, the upper and lower signs correspond to neutrino and anti–neutrino scatterings, respectively. For the charged current reaction of type (ν_l, lN) with lepton mass m_l, each term in the product $\omega_{\mu\nu}W^{\mu\nu}$, Eq. (A10), may be written as

$$\begin{aligned}\omega_L W_L = \frac{1}{4\epsilon_i k_f}\Bigg\{ & \left[(\epsilon_i+\epsilon_f)^2 - |\vec{k}\,|^2 - m_l^2\right]|\rho|^2 \\ & + \left[\frac{(\epsilon_i^2-k_f^2)^2}{|\vec{k}\,|^2} - \omega^2 + m_l^2\right]|J_k|^2 \\ & - \left[\frac{2(\epsilon_i+e_f)(\epsilon_i^2-k_f^2)}{|\vec{k}\,|} - 2\omega|\vec{k}\,|\right] Re\,(\rho^* J_k)\Bigg\}\end{aligned} \tag{A30}$$

$$\begin{aligned}\omega_T W_T = \Bigg\{ & \frac{\epsilon_i k_f \sin^2\theta}{2|\vec{k}\,|^2}\cos(2\phi_F)\Big(|J_\parallel|^2 - |J_\perp|^2\Big) \\ & + \left[\frac{\epsilon_i k_f \sin^2\theta}{2|\vec{k}\,|^2} - \frac{1}{2}\left(\frac{-\epsilon_f}{k_f} + \cos\theta\right)\right]\Big(|J_\parallel|^2 + |J_\perp|^2\Big)\Bigg\}\end{aligned} \tag{A31}$$

$$\begin{aligned}\omega_{LT} W_{LT} = & \frac{\sin\theta}{|\vec{k}\,|}\Big(\epsilon_i+\epsilon_f\Big) \\ & \times Re\left[\left(\frac{\epsilon_i^2-k_f^2}{|\vec{k}\,|(\epsilon_i+\epsilon_f)}J_k^* - \rho^*\right)\Big(J_\parallel\cos\phi_F - J_\perp\sin\phi_F\Big)\right]\end{aligned} \tag{A32}$$

$$\omega_{TT} W_{TT} = -\frac{\epsilon_i k_f \sin^2\theta}{|\vec{k}\,|^2}\sin(2\phi_F) Re\,(J_\perp J_\parallel^*) \tag{A33}$$

$$\omega_{LT'} W_{LT'} = -\sin\theta\; Im\left[\left(\rho^* - \frac{\omega}{|\vec{k}\,|}J_k^*\right)\Big(J_\parallel\sin\phi_F + J_\perp\cos\phi_F\Big)\right] \tag{A34}$$

$$\omega_{TT'} W_{TT'} = -\frac{1}{|\vec{k}\,|}\left(\frac{\epsilon_i\epsilon_f}{k_f} + k_f - (\epsilon_i+\epsilon_f)\cos\theta\right) Im\,(J_\parallel J_\perp^*) \tag{A35}$$

In both the charged and neutral current processes the 4-momentum of the scattered lepton is not observed and it is thus necessary to integrate over the unobserved final lepton 3-momentum $\vec{k}_f$ in addition to the angular variables of the ejected nucleon. This leads to the following differential cross section for *free* nucleons

$$\left(\frac{d\sigma^{Z^0/W^\pm}}{dE_F}\right)_{\text{Free}} = \frac{\sigma^{Z^0/W^\pm}}{4\epsilon_f^2}\frac{2\pi}{|\vec{k}\,|}\Big(\omega_L W_L + \omega_T W_T + \omega_{TT'} W_{TT'}\Big) \tag{A36}$$

In the relativistic FGM, non–interacting nucleons are filled up to the Fermi momentum k_F and the initial momentum of the struck nucleon have to be averaged over the Fermi sphere.

In addition, the initial energy of this nucleon E_I is often reduced with respect to its free space value by the binding energy, expressed by an input parameter B

$$\begin{aligned} E_I &= \left(|\vec{P_I}\,|^2 + M^2\right)^{1/2} - B \\ &= \left(|\vec{k}|^2 + |\vec{P}_F|^2 - 2\,\vec{k}\cdot\vec{P}_F + M^2\right)^{1/2} - B \end{aligned} \tag{A37}$$

The resulting differential cross sections *per nucleon* for neutral and charged current processes in the RFGM are

$$\left(\frac{d\sigma^{Z^0/W^\pm}}{dE_F}\right)_{\rm RFGM} = \left(\frac{3\pi}{4k_F^3}\right)\int_0^{k_F} d\epsilon_f d(\cos\theta)\,\frac{\sigma^{Z^0/W^\pm}}{|\vec{k}\,|}\Big[\omega_L W_L + \omega_T W_T + \omega_{TT'} W_{TT'}\Big] \tag{A38}$$

Integrations over ϵ_f and $\cos\theta$ in Eq. (A38) are performed numerically. For further technical details see [59].

APPENDIX B: TWO–BODY EXCHANGE CURRENT OPERATORS

This Appendix presents the general form for the two–body soft–pion MEC operator, $J^a_\mu(k;P_{I,1};P_{I,2};P_{F,1};P_{F,2})_{EX}$, given in Eq. (2.16) where the probing current, $J^a_\mu(k)$, may be any one of vector or axial $SU(3)$ currents. Since the matrix element for the pion absorption is given by Eq. (2.17), the quantity of interest here are the amplitudes for the soft–pion production shown in Eq. (2.20). Therefore, only these amplitudes are shown explicitly here and the relevant full soft–pion MEC operators for electromagnetic, neutral and charged current scattering reactions may be constructed by taking the appropriate linear combinations of the operators given in this appendix, multiplied by the pion propagator and the πNN vertex function as shown in Eq. (2.16).

Using the notation introduced in the text and in Appendix A, the amplitude for soft–pion production induced by the vector singlet current V^0_μ is found to be

$$\begin{aligned} &\lim_{q\to 0}\langle \pi^a(q)N(P_F)|V^0_\mu(k)|N(P_I)\rangle = \\ &\qquad (-i)\bar{u}(\vec{P}_F,\sigma_F)\Big[V^0_A\gamma_5\gamma_0\gamma_\mu + V^0_B\gamma_5\gamma_\mu\gamma_0 + V^0_C\gamma_5\gamma_0\Sigma_\mu \\ &\qquad\qquad + V^0_D\gamma_5\Sigma_\mu\gamma_0 + V^0_E\gamma_5\Sigma_\mu\Big]\lambda^a u(\vec{P}_I,\sigma_I) \end{aligned} \tag{B1}$$

In the above expression $a = 1,2,3$ for pion production and the coefficients V^0_J multiplying the operators are defined as

$$V^0_A \equiv +\sqrt{\frac{2}{3}}F^0_1(k^2)\left(\frac{g_{\pi NN}}{2E_2}\right) \tag{B2}$$

$$V^0_B \equiv +\sqrt{\frac{2}{3}}F^0_1(k^2)\left(\frac{g_{\pi NN}}{2E_1}\right) \tag{B3}$$

$$V^0_C \equiv +\sqrt{\frac{2}{3}}F^0_2(k^2)\left(\frac{g_{\pi NN}}{2E_2}\right) \tag{B4}$$

$$V^0_D \equiv -\sqrt{\frac{2}{3}}F^0_2(k^2)\left(\frac{g_{\pi NN}}{2E_1}\right) \tag{B5}$$

$$V_E^0 \equiv +\sqrt{\frac{2}{3}} F_2^0(k^2) \left(\frac{g_{\pi NN}}{M}\right) \tag{B6}$$

$$\tag{B7}$$

with $E_i \equiv \sqrt{|\vec{P}_i\,|^2 + M^2}$. The vector singlet amplitude, Eqs. (B1) is divergenceless *when the nucleons are assumed to obey the free Dirac equation*, leading to current conservation for vector singlet MEC. The corresponding vector octet soft–pion production amplitude is

$$\begin{aligned}
&\lim_{q\to 0}\langle \pi^a(q) N(P_F)|V_\mu^b(k)|N(P_I)\rangle = \\
&(+i)\bar{u}(\vec{P}_F,\sigma_F)\left\{\frac{1}{4}\Big[\lambda^a,\lambda^b\Big]_+\Big(V_A^b\gamma_5\gamma_0\gamma_\mu + V_B^b\gamma_5\gamma_\mu\gamma_0 + V_C^b\gamma_5\gamma_0\Sigma_\mu + V_D^b\gamma_5\Sigma_\mu\gamma_0 + V_E^b\gamma_5\Sigma_\mu\Big)\right. \\
&\qquad +\frac{1}{4}\Big[\lambda^a,\lambda^b\Big]_-\Big(V_A^b\gamma_5\gamma_0\gamma_\mu - V_B^b\gamma_5\gamma_\mu\gamma_0 + V_C^b\gamma_5\gamma_0\Sigma_\mu - V_D^b\gamma_5\Sigma_\mu\gamma_0 + V_F^b\gamma_5\gamma_\mu \\
&\qquad\qquad \left. +V_0^c\gamma_5 k_\mu\Big)\right\} u(\vec{P}_I,\sigma_I)
\end{aligned} \tag{B8}$$

where the index b runs from 1 to 8. The coefficients V_J^b are

$$V_A^b \equiv +F_1^b(k^2)\left(\frac{g_{\pi NN}}{E_2}\right) \tag{B9}$$

$$V_B^b \equiv +F_1^b(k^2)\left(\frac{g_{\pi NN}}{E_1}\right) \tag{B10}$$

$$V_C^b \equiv +F_2^b(k^2)\left(\frac{g_{\pi NN}}{E_2}\right) \tag{B11}$$

$$V_D^b \equiv -F_2^b(k^2)\left(\frac{g_{\pi NN}}{E_1}\right) \tag{B12}$$

$$V_E^b \equiv +F_2^b(k^2)\left(\frac{2g_{\pi NN}}{M}\right) \tag{B13}$$

$$V_F^b \equiv +\left(F_1^b(k^2) + \frac{G_A^b(k^2)}{g_A}\right)\left(\frac{2g_{\pi NN}}{M}\right) \tag{B14}$$

$$V_0^b \equiv \left(\frac{F_\pi^b(k^2)}{k^2 - m_\pi^2} - \frac{H_A^b(k^2)}{g_A}\right)(2g_{\pi NN}) \tag{B15}$$

The first term in the coefficient V_0^b yields the "pion–in–flight" MEC with the pion form factor $F_\pi(k^2)^b$. However, this "pion–in–flight" term is proportional to the four momentum transfer of the leptonic probe, k_μ, and thus does not contribute to the neutral current total cross section. It also does not contribute to the electron scattering total cross section when the usual approximation of neglecting the electron mass is made. Terms proportional to k_μ also do not contribute to the (e,e') longitudinal and transverse response functions R_L and R_T, when they are evaluated by using all the components of the electromagnetic four current as done in this paper. The coefficient V_0^b can be made to vanish by assuming a point like pion and using the pion pole dominance approximation from PCAC, Eq. (3.1). For momentum transfers ranging from β–decay to the quasi–elastic kinematics where the soft–pion MEC operators are applicable, this should be a good approximation.

However, even when V_0^b is made to vanish the vector octet soft–pion production amplitude, Eq. (B8), is not divergenceless. The problem is the term with coefficient V_F^b which

has the structure of an axial current. The prescription used by Adler [46] to make Eq. (B8) divergenceless and thus guarantee the conservation of vector currents involves adding appropriate counter terms proportional to k_μ. In the present case, this counter term is $V_G^b \gamma_5 k_\mu$ where V_G^b is given by

$$V_G^b \equiv + \left(\frac{G_A^b(k^2)}{g_A} \right) \left(\frac{4 g_{\pi NN}}{k^2} \right) \tag{B16}$$

This prescription is applicable to neutral current and electromagnetic reactions since terms proportioinal to k_μ do not contribute to the total cross sections. However, it leads to ambiguities for the charged current reactions where one of the leptons is massive and terms proportional to k_μ in the hadronic current must explicitly be taken into account in the derivation of the reaction cross section. Nevertheless, since the generalized soft–pion dominance method of Chemtob and Rho ought to be applicable for all types of currents, it is desirable to insure the conservation of vector currents in this manner. In the present application, the contribution from the counter term $V_G^b \gamma_5 k_\mu$ to the charged current cross section was found to be numerically very small (about 1% of the total MEC contribution).

The matrix element of interest for the probing axial singlet current may be written as

$$\begin{aligned} &\lim_{q\to 0} \langle \pi^a(q) N(P_F) | A_\mu^0(k) | N(P_I) \rangle = \\ &\quad (+i) \bar{u}(P_F, \sigma_F) \Big[A_A^0 \gamma_0 \gamma_\mu + A_B^0 \gamma_\mu \gamma_0 + A_C^0 k_\mu + A_D^0 \gamma_0 k_\mu \Big] \lambda^a u(P_I, \sigma_I) \end{aligned} \tag{B17}$$

where,

$$A_A^0 \equiv + \sqrt{\frac{2}{3}} G_A^0(k^2) \left(\frac{g_{\pi NN}}{2 E_2} \right) \tag{B18}$$

$$A_B^0 \equiv - \sqrt{\frac{2}{3}} G_A^0(k^2) \left(\frac{g_{\pi NN}}{2 E_1} \right) \tag{B19}$$

$$A_C^0 \equiv + \sqrt{\frac{2}{3}} H_A^0(k^2) \left(\frac{g_{\pi NN}}{M} \right) \tag{B20}$$

$$A_D^0 \equiv - \sqrt{\frac{2}{3}} H_A^0(k^2) \left(\frac{g_{\pi NN}}{2} \right) \left(\frac{1}{E_1} + \frac{1}{E_2} \right) \tag{B21}$$

Similarly, the corresponding amplitude for the axial octet current is

$$\begin{aligned} &\lim_{q\to 0} \langle \pi^a(q) N(P_F) | A_\mu^b(k) | N(P_I) \rangle = \\ &(+i) \bar{u}(P_F, \sigma_F) \left\{ \frac{1}{4} \Big[\lambda^a, \lambda^b \Big]_+ \Big(A_A^b \gamma_0 \gamma_\mu + A_B^b \gamma_\mu \gamma_0 + A_C^b \gamma_0 k_\mu + A_D^b k_\mu \Big) \right. \\ &\quad \left. + \frac{1}{4} \Big[\lambda^a, \lambda^b \Big]_- \Big(A_A^b \gamma_0 \gamma_\mu - A_B^b \gamma_\mu \gamma_0 + A_E^b \gamma_0 k_\mu + A_F^b (p_1 + p_2)_\mu + A_G^b \gamma_\mu \Big) \right\} u(P_I, \sigma_I) \end{aligned} \tag{B22}$$

with the following coefficients

$$A_A^b \equiv + G_A^b(k^2) \left(\frac{g_{\pi NN}}{E_2} \right) \tag{B23}$$

$$A_B^b \equiv -G_A^b(k^2)\left(\frac{g_{\pi NN}}{E_1}\right) \tag{B24}$$

$$A_C^b \equiv -H_A^b(k^2) g_{\pi NN}\left(\frac{1}{E_1}+\frac{1}{E_2}\right) \tag{B25}$$

$$A_D^b \equiv +H_A^b(k^2)\left(\frac{2g_{\pi NN}}{M}\right) \tag{B26}$$

$$A_E^b \equiv -H_A^b(k^2) g_{\pi NN}\left(\frac{1}{E_2}-\frac{1}{E_1}\right) \tag{B27}$$

$$A_F^b \equiv +F_2^b(k^2)\left(\frac{g_{\pi NN}}{g_A M^2}\right) \tag{B28}$$

$$A_G^b \equiv -\Big(F_1^b(k^2)+F_2^b(k^2)+g_A G_A^b(k^2)\Big)\left(\frac{2g_{\pi NN}}{g_A M}\right) \tag{B29}$$

Note that it is straightforward to generalize these soft–pion production amplitudes to pseudoscalar octet soft–meson production amplitudes where the $SU(3)$ index a now takes on values from 1 to 8 and the πNN coupling constant is replaced by the appropriate meson–nucleon coupling constants. However, in deriving the above amplitudes the Goldberger–Trieman relation was used to simplify the expressions and this algebraic manipulation is not necessarily justifiable for other pseudoscalar octet mesons under consideration.

REFERENCES

[1] *Mesons in Nuclei*, Vol. 2, edited by M. Rho and D. Wilkinson (North Holland, Amsterdam, 1979).
[2] D.O. Riska, Phys. Rep. **181**, 207 (1989).
[3] B. Frois and J.F. Mathiot, Comments Part. Nucl. Phys. **18**, 291 (1989).
[4] A.J.F. Siegert, Phys. Rev. **37**, 786 (1937).
[5] D.O. Riska and G.E. Brown, Phys. Letts. **B38**, 193 (1972).
[6] J. Hockert, D.O. Riska, M. Gari and A. Huffman, Nucl. Phys. **A217**, 14 (1973).
[7] J.I. Fujita and M. Hirata, Phys. Letts. **37B**, 237 (1971).
[8] J. Dubach, J.H. Koch and T.W. Donnelly, Nucl. Phys. **A271**, 279 (1976).
[9] J.W. Van Orden and T.W. Donnelly, Ann. Phys. (NY) **131**, 451 (1981).
[10] M.J. Dekker, P.J. Brussaard and J.A Tjon, Phys. Letts. **266B**, 249 (1991).
[11] M.J. Dekker, *Relativistic Meson Exchange And Isobar Currents in Electron Scattering*, PhD. Thesis, University of Utrecht (1993) (unpublished).
[12] J. Ryckebusch, *et al.*, Nucl. Phys. **A568**, 828 (1994).
[13] K. Kubodera, J. Delorme and M. Rho, Phys. Rev. Lett. **40**, 755 (1978).
[14] P. Guichon, M. Giffon and C. Samour, Phys. Lett. **B74**, 15 (1978).
[15] E.K. Warburton, Phys. Rev. Letts. **66**, 1823 (1991).
[16] E.K. Warburton and I.S. Towner, Phys. Letts. **B294**, 1 (1992).
[17] E.K. Warburton, I.S. Towner and B.A. Brown, Phys. Rev. C **49**, 824 (1994).
[18] L.A. Ahrens, *et.al.*, Phys. Rev. D **35**, 785 (1987).
[19] D.B. Kaplan and A. Manohar, Nucl. Phys. **B310**, 527 (1988).
[20] T. Suzuki, Y. Kohyama and K. Yazaki, Phys. Letts. **B252**, 323 (1990).
[21] E.M. Henley, G. Grein, S.J. Pollock and A.G. Williams, Phys. Letts. **B269**, 31 (1991).
[22] G. Garvey, S. Krewald, E. Kolbe and K. Langnake, Phys. Letts. **B289**, 249 (1992).
[23] E. Kolbe, K. Langanke, S. Krewald and F.K. Thielmann, Ap. J. **401**, L89 (1992).
[24] G. Garvey, E. Kolbe and K. Langnake, Phys. Rev. C **48**, 1919 (1993).
[25] C.J. Horowitz, H. Kim, D.P. Murdock and S. Pollock, Phys. Rev. C **48**, 3078 (1993).
[26] J. Ashman *et al.*, Phys. Letts. **B206**, 364 (1988); Nucl. Phys. **B328**, 1 (1989).
[27] For an up–to–date bibliography on this issue see J. Ellis and M. Karliner, Report No. hep–ph/9407287.
[28] M.J. Musolf *et al.*, Physics Reports **239**, 1 (1994).
[29] S.L. Mintz and D.F. King, Phys. Rev. C **30**, 1585 (1984).
[30] M. Albert *et al.*, Report No. nucl–th/9410039.
[31] E. Kolbe, K. Langanke and S. Krewald, Phys. Rev. C **49**, 1122 (1994).
[32] W. Müller and M. Gari, Phys. Letts. **B102**, 389 (1981).
[33] S.K. Singh and H. Arenhövel, Z. für Phys. **A324**, 347 (1986).
[34] J.N. Bachall, K. Kubodera and S. Nozawa, Phys. Rev. D **38**, 1030 (1988).
[35] N. Tatara, Y. Kohyama and K. Kubodera, Phys. Rev. C **42**, 1694 (1990).
[36] Y. Umino, J.M. Udias and P.J. Mulders, Phys. Rev. Letts. **74**, 4993 (1995).
[37] J.M. Udias and Y. Umino, work in progress.
[38] E.J. Beise and R.D. McKeown, Comm. Nucl. Part. Phys., **20**, 105 (1990)
[39] M. Chemtob and M. Rho, Nucl. Phys. **A163**, 1 (1971).

[40] M. Bernheim, *et al.*, Phys. Rev. Letts. **46**, 402 (1981).
[41] M. Rho and G.E. Brown, Comments Nucl. Part. Phys. **10**, 201 (1981).
[42] M. Rho, Phys. Rev. Letts. **66**, 1275 (1991).
[43] S. Weinberg, Physica **96A**, 327 (1979).
[44] S. Weinberg, Phys. Letts. **B251**, 288 (1990).
[45] T.-S. Park, I.S. Towner and K. Kubodera, Nucl. Phys. **A579**, 381 (1994).
[46] S.L. Adler, Ann. Phys. (NY) **50**, 189 (1968).
[47] S.L. Adler, Phy. Rev. **139**, 1638 (1965).
[48] J.W. Van Orden, Ph.D. Thesis, Stanford University, 1978 (unpublished).
[49] W.M. Alberico *et al.*, Phys. Rev. **C38**, 1801 (1988).
[50] P. Barreau *et al.*, Nucl. Phys. **A402**, 515 (1983).
[51] G. Orlandini and M Triani, Rep. Prog. Phys. **54**, 257 (1991).
[52] M. Kohno and N. Ohtsuka, Phys. Letts. **B98**, 335 (1981).
[53] D.D. Koetke *et al.*, Phys. Rev. C **46**, 2554 (1992).
[54] B. Bodmann *et al.*, Phys. Letts. **B280**, 198 (1992).
[55] Los Alamos National Laboratory Proposal, LA–11842–P, August 1990.
[56] H. Kim, J. Piekarewicz and C.J. Horowitz, Report- No. nucl-th/9412017.
[57] H. Kim, J. Piekarewicz and C.J. Horowitz, Report No. nucl–th/9502041.
[58] F. Halzen and A.D. Martin, *Quarks and Leptons*, (John Wiley and Sons, N.Y., 1984).
[59] J.M. Udias, NIKHEF–K Internal report (1995), NIKHEF–K 95–P12.

FIGURE CAPTIONS

FIG 1. a) Longitudinal, R_L, and b) transverse, R_T, response functions for the $^{12}C(e,e')$ reaction plotted against the energy transfer ω. The three momentum transfer involved in the inclusive reaction is $|\vec{k}\,| = 400$ MeV. A RFG model without any binding energy corrections ($B = 0$) and with a Fermi momentum of $k_F = 225$ MeV was used to calculate the response functions . Experimental data, taken from [50], are shown for reference but no attempt to fit the data by varying B and k_F has been made. The dashed line represents the impulse approximation results while response functions obtained with soft–pion MEC corrections are shown with solid lines. Also shown in the figures using the dashed-dotted lines are the individual contributions from soft–pion two–body courrents.

FIG 2 $^{12}C(\nu_{\mu^-},\mu^-)X$ total cross section obtained by folding the LSND neutrino flux [30] versus the Fermi momentum k_F. The dashed curve is the impulse approximation result while the solid curve is obtained with the soft–pion MEC corrections using the RFG model of the nucleus with no binding energy correction ($B = 0$). For $k_F = 225$ MeV, which is the usual value used for ^{12}C, the total cross–section is reduced from 24 to 22.7 ($\times 10^{-40}$cm^2) when corrected for two–body current effects.

FIG. 3 a) $^{12}C(\nu_{\mu^-},\mu^-)X$ total cross section as a function of incoming neutrino energy E_ν taking into account the Coulomb correction for the outgoing muon. As in Figure 2, the RFG model is used to model the nucleus with $k_F = 225$ MeV and $B = 0$. The dashed line is the impulse approximation result while the solid line includes two–body soft–pion MEC effects. Note that in this particular case there is very little difference between the two results. b) Differential cross section $d\sigma/dE_\mu$ for the same process obtained with and without the soft–pion MEC correction plotted against the outgoing muon kinetic energy E_μ. The results for this figure is obtained by folding the LSND neutrino energy distribution obtained from [30].

FIG 4 $^{12}C(\nu,\nu'p)$ differential cross section versus the kinetic energy of the ejected nucleon, T_F, for a) $k_F = 200$ MeV, b) $k_F = 300$ MeV and c) $k_F = 350$ MeV. The incident neutrino energy is assumed to be 200 MeV while the values for the strange quark form factors used are $F_2^s = -0.21$ and $G_A^s = -0.19$. The long dashed curve is the impulse approximation result while the solid curves have been obtained with soft–pion MEC corrections.

FIG. 5 $^{12}C(\nu,\nu'p)$ differential cross section versus the kinetic energy of the ejected nucleon, T_F, with ($F_2^s = -0.21$ and $G_A^s = -0.19$) and without finite strange quark form factors. The incident neutrino energy is assumed to be 200 MeV and the long dashed curve is the impulse approximation result while the solid curves have been obtained with soft–pion MEC corrections.

FIG. 6 Various structure function contributions to the $^{12}C(\nu,\nu'p)$ differential cross sec-

tion shown in Figure 5. Both the impulse approximation and MEC corrected results for the transverse, $\omega_T W_T$, longitudinal, $\omega_L W_L$, and transverse–transverse, $\omega_{TT'} W_{TT'}$, contributions are shown explicitly using the dashed and solid lines, respectively. Note that the two–body corrected contributions from the transverse and transverse–transverse contributions cancel leading to a small overall MEC correction to the impulse approximation. For anti–neutrino scattering the transverse–transverse contribution changes sign resulting in a smaller differential cross section but in a larger MEC effect compared to neutrino scattering.

FIG. 7 $^{12}C(\nu, \nu' p)$ and $^{12}C(\bar{\nu}, \bar{\nu}' p)$ differential cross sections versus the kinetic energy of the ejected nucleon, T_F. The incident neutrino energy is 200 MeV and the nucleon is assumed to have strange quark form factors of $F_2^s = -0.21$ and $G_A^s = -0.19$. The long dashed curve is the impulse approximation result while the solid curves have been obtained with soft–pion MEC corrections.

FIG. 8 a) Ratios of integrated proton–to–neutron quasi–elastic yield for the $^{12}C(\nu, \nu' N)$ reaction as functions of G_A^s for two values of strange magnetic form factor F_2^s. In each case, the dashed line is the impulse approximation result while the solid line has been corrected for meson exchange currents. The incident neutrino energy is assumed to be 200 MeV for both cases and the range of integration was chosen to be $50 \leq T_F \leq 120$ MeV to simulate the LSND experiment [22]. b) Same as in a) but for anti–neutrino scattering.

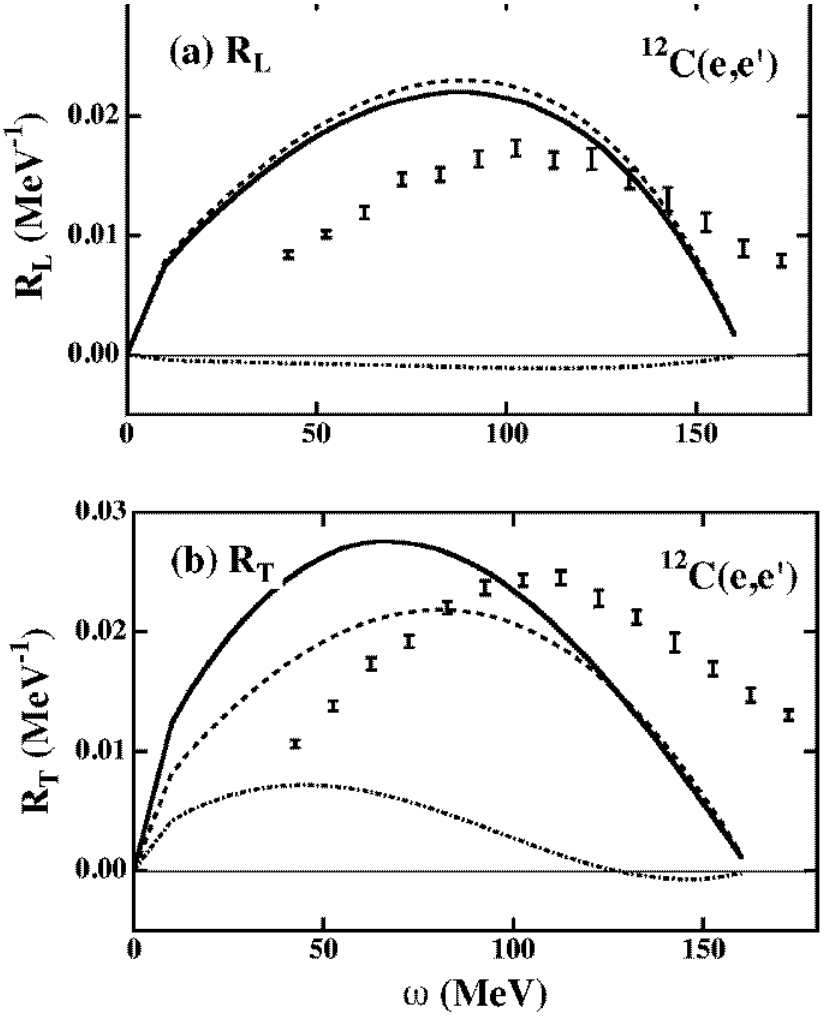
(a) R_L
$^{12}C(e,e')$
R_L (MeV^{-1})
0.02
0.01
0.00
0
50
100
150
(b) R_T
$^{12}C(e,e')$
R_T (MeV^{-1})
0.03
0.02
0.01
0.00
0
50
100
150
ω (MeV)

Figure 1

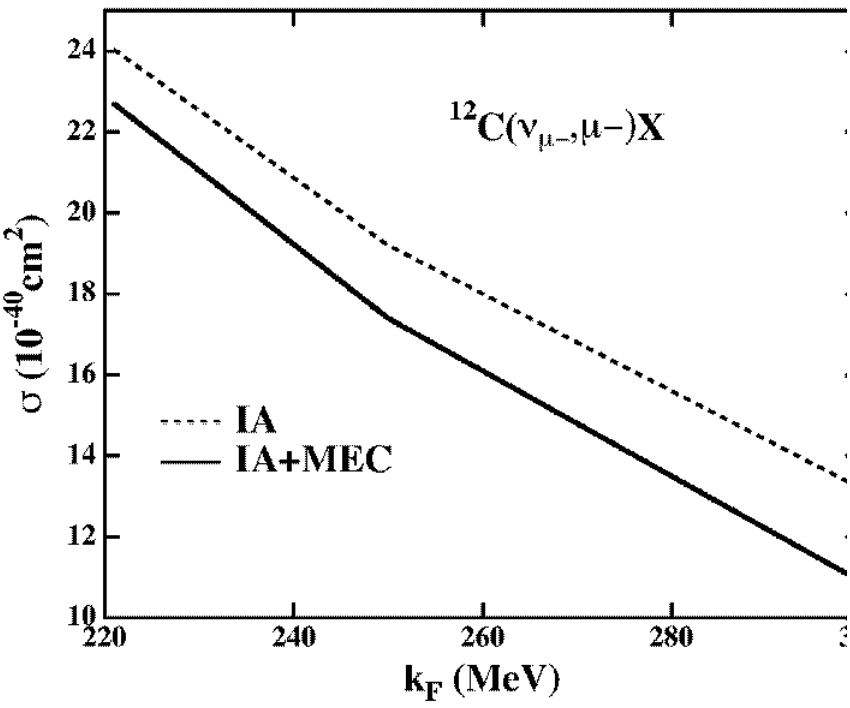
$^{12}C(\nu_{\mu-},\mu-)X$
IA
IA+MEC
σ ($10^{-40}cm^2$)
k_F (MeV)
24
22
20
18
16
14
12
10
220
240
260
280

Figure 2

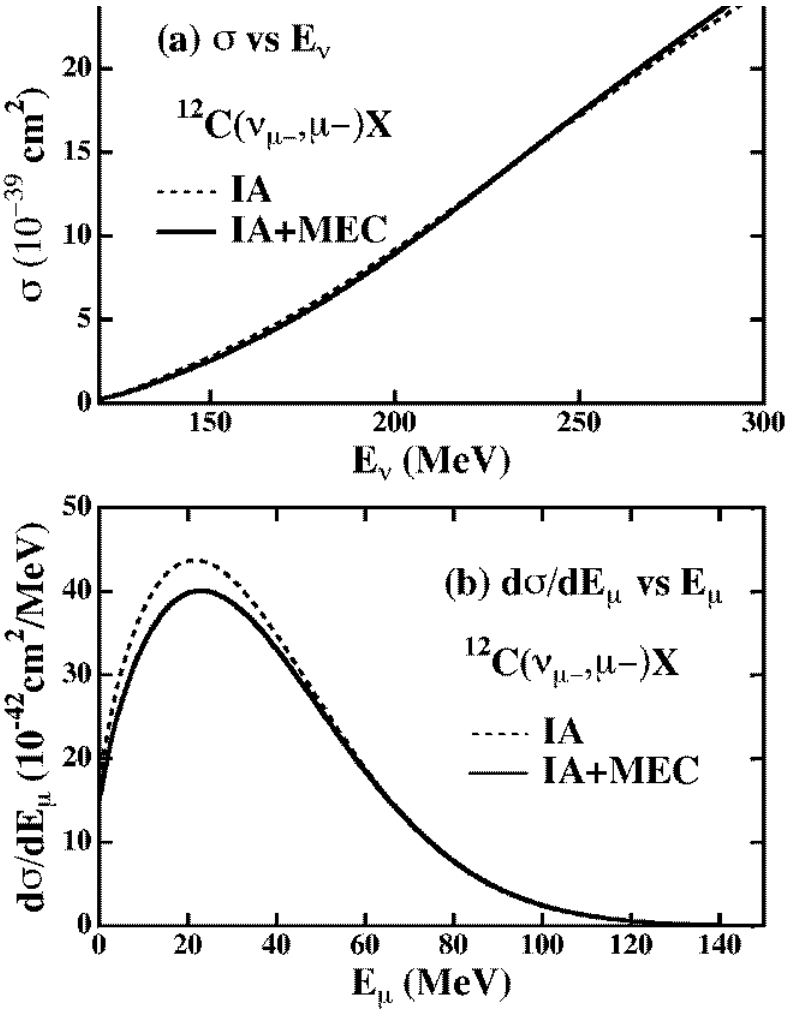
(a) σ vs E_ν
$^{12}C(\nu_{\mu-},\mu-)X$
IA
IA+MEC
σ (10^{-39} cm^2)
E_ν (MeV)
(b) dσ/dE_μ vs E_μ
$^{12}C(\nu_{\mu-},\mu-)X$
IA
IA+MEC
dσ/dE_μ ($10^{-42}$$cm^2$/MeV)
E_μ (MeV)

Figure 3

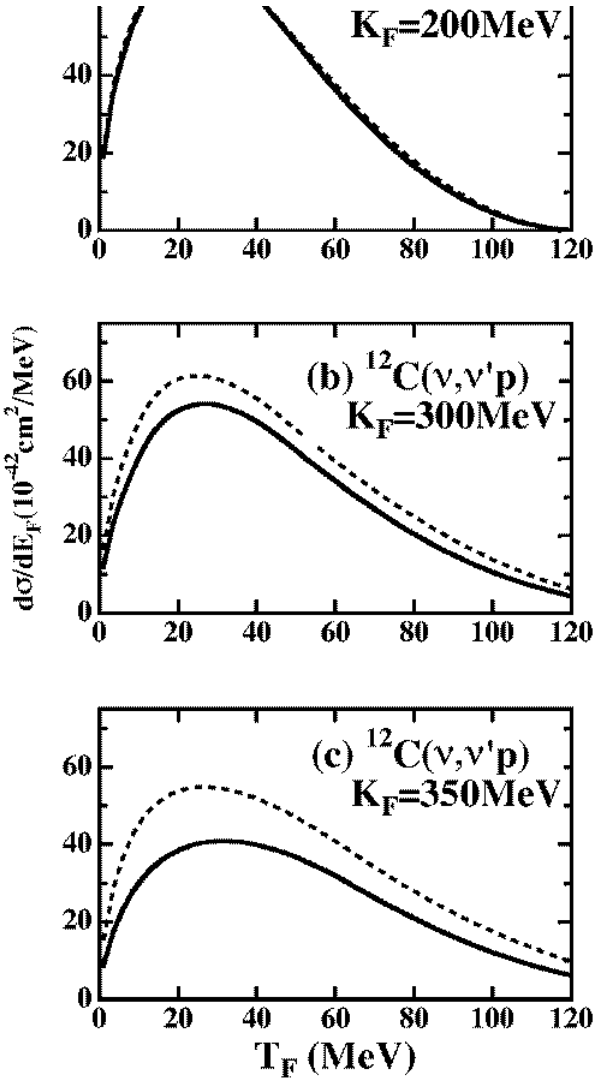
K_F=200MeV
(b) ^12C(ν,ν'p)
K_F=300MeV
(c) ^12C(ν,ν'p)
K_F=350MeV
dσ/dE_F(10^-42 cm^2/MeV)
T_F (MeV)
0
20
40
60
80
100
120

Figure 4

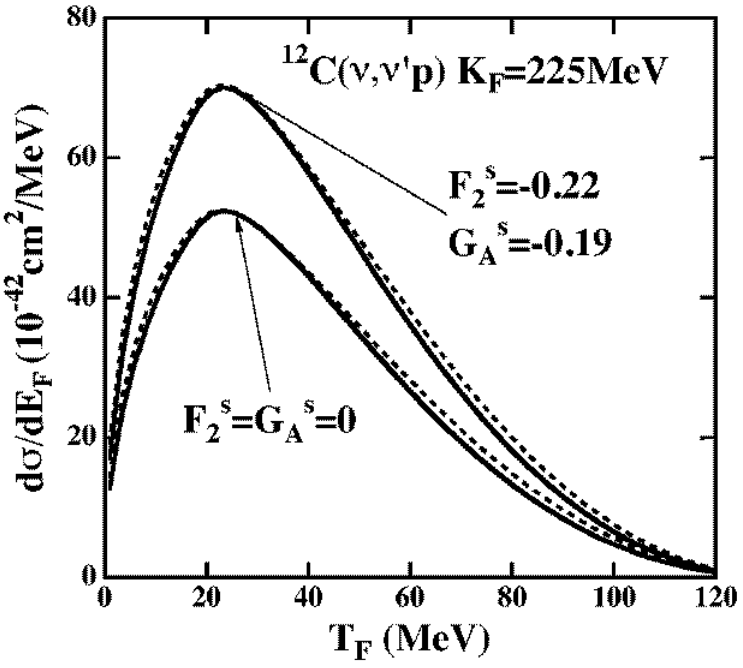
$^{12}C(\nu,\nu'p)$ K_F=225MeV
F_2^s=-0.22
G_A^s=-0.19
F_2^s=G_A^s=0
$d\sigma/dE_F$ ($10^{-42}cm^2$/MeV)
T_F (MeV)
0
20
40
60
80
100
120

Figure 5

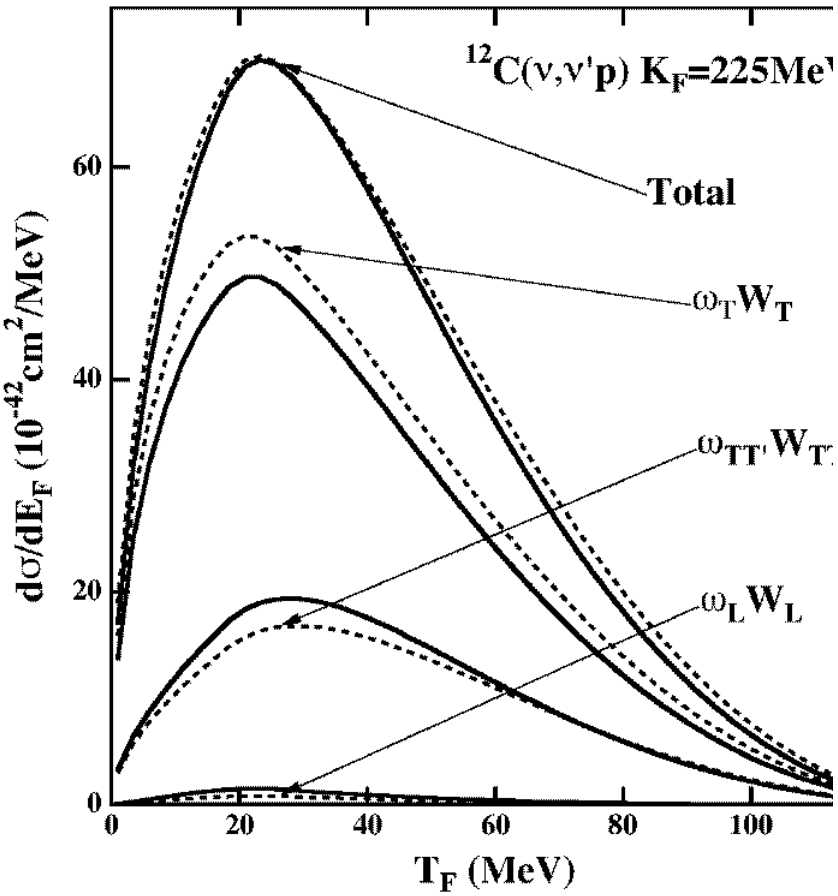
^{12}C(ν,ν'p) K$_F$=225Me
Total
ω$_T$W$_T$
ω$_{TT'}$W$_{T'}$
ω$_L$W$_L$
dσ/dE$_F$ (10^{-42}cm^2/MeV)
T$_F$ (MeV)
0
20
40
60
80
100

Figure 6

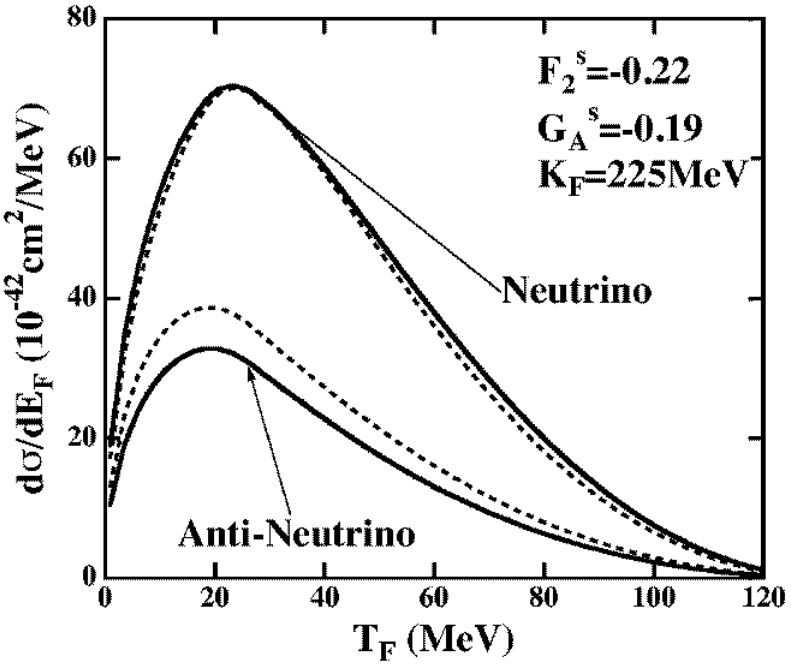
80
60
40
20
0
0
20
40
60
80
100
120
F_2^S=-0.22
G_A^S=-0.19
K_F=225MeV
Neutrino
Anti-Neutrino
$d\sigma/dE_F$ ($10^{-42}cm^2$/MeV)
T_F (MeV)

Figure 7

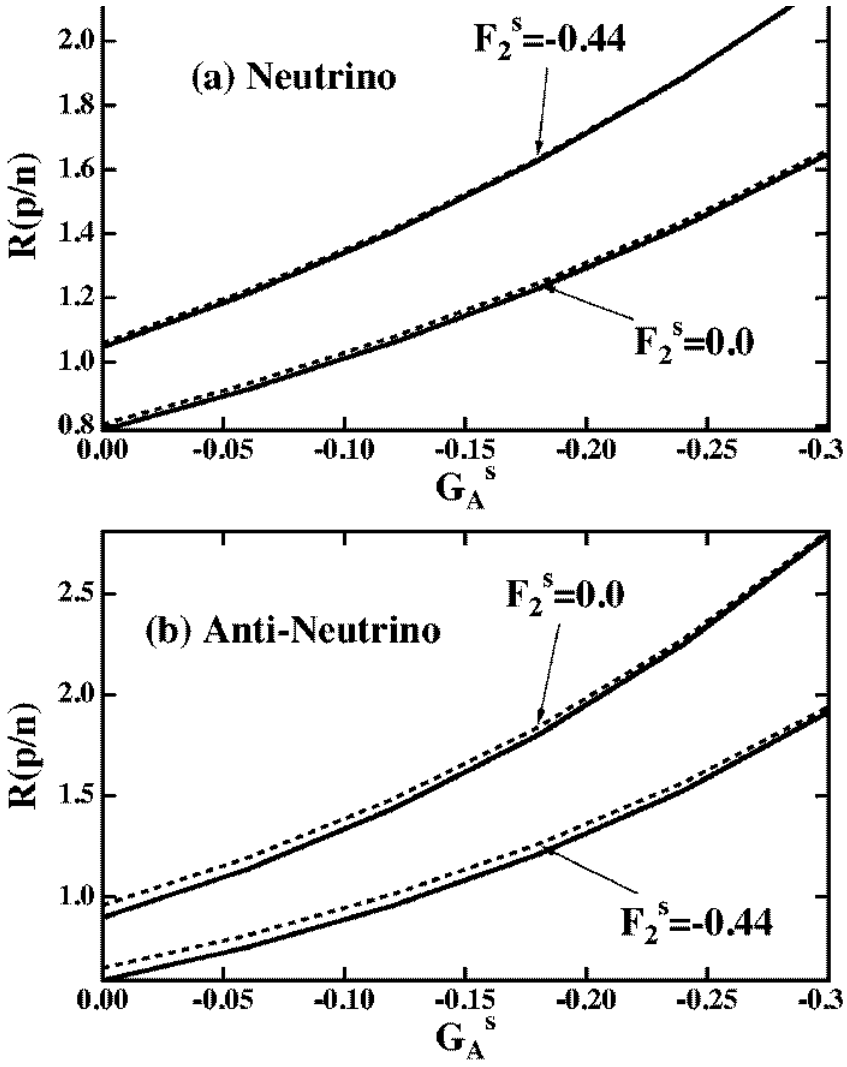
(a) Neutrino
F_2^s=-0.44
F_2^s=0.0
R(p/n)
G_A^s
(b) Anti-Neutrino
F_2^s=0.0
F_2^s=-0.44
R(p/n)
G_A^s

Figure 8